AN ABSTRACT OF THE THESIS OF

Adnan Morkoc for the degree of Master of Science in Water Resources Engineering presented on November 6, 2019

Title: Modeling and Validation of Denitrification Bioreactors for Agricultural Tile Drainage

Abstract approved:

_____

Frank W.R. Chaplen

Agricultural tile drainage is one of the major causes of increasing nitrate (NO_3^-) concentrations in surface water bodies thanks to the usage of nitrogen fertilizers and manure. Denitrifying bioreactors are constructed at the edge of agricultural lands in order to remove NO_3^- from drainage water through labile carbon substrates intended to promote denitrification.

This field-scale study is the examination and modeling of NO_3^- removal performance of a woodchip bioreactor installed in Corvallis, OR. During flow periods, water samples were collected on a weekly basis for lab analysis of nitrate, nitrite and ammonium. NO_3^- concentrations measured in the influent varied in the range from 2 to 13 mg/L (on average 8 mg/L) while effluent concentrations averaged 6 mg/L (1 - 12 mg/L). Results showed that mean volumetric NO_3^- removal rate achieved by the bioreactor throughout the study period was 21 g N/ m^3 /d and the average percent NO_3^- reduction was 26% that fell within the range of reported values. These findings further indicated that

woodchip bioreactors operating under cold-weather environmental settings are effective means to removal of NO_3^- loads from agricultural landscapes.

The model that integrates simulated drainage discharge into temperature-dependent denitrification rates was validated using observed effluent nitrate with a Nash-Sutcliffe efficiency coefficient (NSE) value of 0.506, indicating the efficacy of the model in line with model evaluation criteria. Based on the univariate analysis conducted, the most sensitive model parameters are influent nitrate, hydraulic retention time and water temperature, respectively.

The MIN3P code was also utilized to predict NO_3^- concentrations along the length of the bioreactor for a simulation interval of a day and nitrate levels in effluent water through the monitoring period. The simulated nitrate concentration profile suggests that nitrate removal occurs primarily within the first few meters of the denitrification bed. The assessment of MIN3P model resulted in a NSE value of 0.043 and a coefficient of determination (R^2) of 0.416.

Modeling and Validation of Denitrification Bioreactors for Agricultural Tile Drainage

by
Adnan Morkoc

A THESIS

submitted to

Oregon State University

in partial fulfillment of
the requirements for the
degree of

Master of Science

Presented November 6, 2019
Commencement June 2020

Master of Science thesis of Adnan Morkoc presented on November 6, 2019

APPROVED:

Major Professor, representing Water Resources Engineering

Director of the Water Resources Graduate Program

Dean of the Graduate School

I understand that my thesis will become part of the permanent collection of Oregon State University libraries. My signature below authorizes release of my thesis to any reader upon request.

Adnan Morkoc, Author

ACKNOWLEDGEMENTS

I would like to express my sincere appreciation to my adviser, Dr. Frank Chaplen, for his guidance, patience and precious technical assistance during idea generation. It would not have been possible to have executable models and to conduct water quality laboratory analysis without his troubleshooting support. Thank you to my committee members, Dr. Todd Jarvis and Dr. Tyler Radniecki for their feedback and willingness to give me good counsel from the beginning of this journey. Thank you to Dr. Marry Santelmann for being eager to help me as the best director and excellent role model to whom wish to be a part of the Water Resources Graduate Program. Thank you to Dr. John Selker for giving me a chance to pursue my higher education at Oregon State University. Thank you to the design team for sharing their field-monitoring data of the bioreactor with me. Thank you to the Biological and Ecological Engineering department staff for being thoughtful, friendly and always taking solution-oriented approach. Finally, I would like to especially thank you to my family for always believing in me and being a phone call away to be my biggest support unconditionally no matter what.

TABLE OF CONTENTS

LIST OF FIGURES

LIST OF FIGURES (Continued)

Figure Page

LIST OF TABLES

LIST OF APPENDIX TABLES

Table Page

Modeling and Validation of Denitrification Bioreactors for Agricultural Tile Drainage

CHAPTER 1. INTRODUCTION

Increasing trends in intensive agricultural practices have had a profound effect on the nitrogen content and the quality of surface water bodies throughout many regions of the United States. Applied nitrogen-based fertilizers are amenable to being washed out from the cultivated soils, since nitrate has highly mobile characteristics in water and soils. Elevated concentrations of nutrients and pesticides, nonpoint source pollution in waterways are mostly attributed to the misapplication and/or overuse of fertilizer and animal waste to cultivated fields through agricultural drainage systems (Scavia & Bricker, 2006). Nitrogen fertilizers have been benefited in modern and intensive agriculture in order to improve crop yields; however, excess nitrogen (N) cannot be taken up by the roots of plants. NO_3^- leaches through soils to surface water bodies and groundwater, reducing soil minerals, acidifying soils, and altering drinking water ecosystems (Likens et al., 1996).

Heavy discharges of NO_3^- into an aquatic system lead to eutrophication, which is likely to cause unintended fertilization of algae blooms that are greater than a given aquatic system can sustain. In addition to eutrophication, the existence of sufficient phosphorus and inorganic nitrogen can result in acidification in freshwater ecosystems as well (D. W. Schindler et al., 1985). Decreased diversity of both animal and plant species, broadly speaking, accompanies both eutrophication and acidification (Schindler, 1990).

Agricultural tile drainage systems are one of the best solutions to enhance

productivity by improving the timeliness of field activities and operability of the soil in many locations around the globe. Subsurface drainage systems, also known as 'tile' drainage, made of water permeable drainage pipes that are typically 10-16 cm in diameter and installed often 0.6 to 1.2 m below poorly drained agricultural land at a gently sloping gradient of 0.01% to 0.1% towards the outlet point(s). These systems are one of the best management practices to improve the soil storage capacity and crop yield. On the other hand, the usage of tile drainage systems is likely to precipitate detrimental water quality problems associated with an outflow of drainage pipes where the excess amount of water collected from the field reaches a local discharge point. Through poorly-managed subsurface drainage systems, dangerous amounts of nitrate are transferred from drainage effluent to local surface water bodies. Before reaching a drainage system, NO_3^- concentration of the water will decrease through soil profile, but drainage water is relatively conveyed rapidly in the pipes. This relatively limited period can impede certain natural processes like denitrification and root uptake to occur in the root zone of the soil (Kellman, 2005). The adverse effects detected on downstream water quality resulted from intensive agricultural applications such as subsurface drainage systems, overuse of fertilizer and animal waste, and irrigation call for best management practices for nitrate removal.

The term of best management practices (BMP) is described as applications which are intended to control the amount of point and/or non-point source pollutants contaminating surface water bodies. The success of these implementations can be evaluated according to their potential to diminish the presence of a nutrient contaminant and how the application alters the mass distribution of the contaminant between sediment,

run-off water and percolating water (Logan, 1993). There are a number of agricultural management strategies used in NO_3^- removal include (1) improved on-field applications such as better crop rotations, cover crops and enhanced fertilizer applications (2) constructed practices such as controlled drainage systems; and (3) edge-of-field or in-stream nitrogen sinks like constructed wetlands and denitrification bioreactors. (Christianson & Helmers, 2011). A combination of two or more such applications and management practices is likely to be required at many fields so that landowners can meet water quality goals in conjunction with satisfactory crop yields. The great variability in the effectiveness of these practices is directly associated with the location of the system as well as temporally alterations in the amount of tile flow and nitrate concentrations. Edge-of-field techniques have particular difficulty decreasing NO_3^- load during high flow periods, and this is when most transport is expected to occur (Ikenberry et al., 2014; Royer et al., 2006).

Denitrification bioreactors for agricultural drainage are an edge-of-field best management practice that involve solid carbon substrates (often fragmented wood-products) are placed into the flow path of tile/drain discharge. The constructed denitrifying bioreactor involve the filtering of nitrate-rich water under an anaerobic condition in order for nitrate-nitrogen (NO_3^--N) removal to occur in drainage effluent through denitrifying bacterial organisms cultivated within the system. In this anaerobic environment electrons donated from carbon media provides the required cellular energy for denitrifiers to proceed the conversion of nitrate to either nitrous oxide (N_2O) or molecular nitrogen (N_2). The most widely approach to define the nitrate attenuation process in the subsurface flows is the heterotrophic denitrification, which includes the reduction of NO_3^- to nitrogen gases

with the help of a carbon source as the electron donor and for growth (Rivett et al., 2008; Seitzinger et al., 2006). The availability of degradable carbon source makes the denitrification reaction possible on the pathway of the subsurface drainage flows before it enters aquatic environments. To date, it has been reported in the literature that there is no necessity to inoculate the soil with denitrifying bacteria since denitrifiers are expected to colonize solid-state carbon media naturally. A wide range of NO_3^- reduction performance (up to 98% NO_3^- attenuation) has been reported in both field-scale studies and laboratory trials over the past decade, particularly in the Midwestern United States (Bell et al., 2015; Christianson et al., 2012; Verma et al., 2010). On the other hand, there is still a lack of information regarding the NO_3^- removal efficiency of bioreactors across different climates, site-specific parameters like soil and drainage conditions and possible unintended side effects such as sulfate reduction and the methylation of mercury.

In the current field scale study reported herein, a recently constructed denitrifying bioreactor at the Oregon State University Experimental Dairy Farm was monitored from December 7, 2017 to February 14, 2018 for its effectiveness to reduce nitrogen contaminants in subsurface tile drainage water. The primary objectives of this project included: (1) determine the amount and percentage removal rate of NO_3^- reduced by the denitrification bioreactor at the OSU dairy farm; (2) predict the tile drain discharge rate entering the bioreactor through, Drainmod (Skaggs, 1978), a widely acknowledged field-scale agricultural drainage and water balance model; (3) simulate nitrate concentration of a denitrification bed effluent with the help of daily drainage rate estimated by Drainmod and, macromolecular rate theory (MMRT) (Hobbs et al., 2013), a thermodynamic theory that incorporates heat capacity into the rate equation to model the temperature dependence of

enzyme reaction rates and microbial growth; and (4) develop simulated NO_3^- concentration profile of the bioreactor via MIN3P (Mayer et al., 2002) which is a powerful three-dimensional analysis tool to simulate multicomponent reactive transport occurring in both the vadose zone and saturated groundwater environment.

CHAPTER 2. LITERATURE REVIEW

2.1 Agricultural Drainage

Artificial drainage systems in modern and intensive agriculture are concerned with removing drainable or standing water from agricultural fields and lowering water table with the help of subsurface perforated pipes and/or surface ditches. Subsurface drainage is a fundamental water management practice for lands where the soil water-permeable enough to allow proper spacing of the drains. The spacing and the depth of corrugated tiles affects the water table level between drains after a rainfall event. The required drainage layout and depth to keep the groundwater level at an optimal value by site-specific parameters like permeability of the soil or topography. Before installing of an entire subsurface drainage system, it is required to survey topography of the field to be drained. The amount of the surveying depends to a great degree upon the lay of the site. Unlike the fields that have a virtually constant slope through the whole land, a topographic survey ought to be done for even slightly undulating areas, otherwise, it would be challenging to decide on the locations where drains should be placed. In addition to topographic information, the drainage layout that best fits the topography of the site is ought to be selected based on a good understanding and drainage characteristics of the soil profile. The four basic patterns used in the design of drainage are illustrated in figure 2.1.

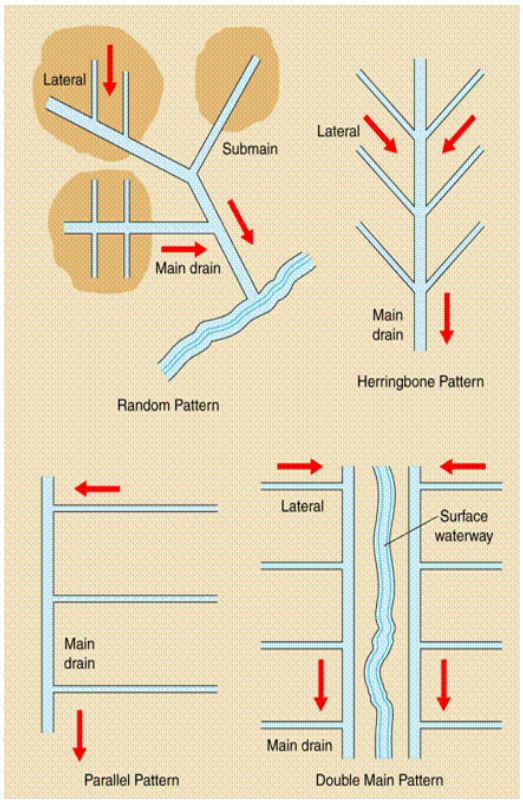

Figure 2.1: Basic patterns for subsurface drainage systems (Drablos & Moe, 1984)

Subsurface drainage systems can be employed with ideal efficiency when approximately half of the total soil volume made out of a continuous network of large and small pores (Drablos & Moe, 1984).

Historically, the most common material for agricultural drainage lines benefited by both the drainage contractor and landowner was clay pipes, typically called tiles, which are inserted end-to-end within trenches. At present, tiles have been replaced with plastic pipes with adequate perforations because of its higher durability and accessibility compared to other possible options made out of clay, concrete, bituminized fiber or metal. These systems enable the landowner to control the cropland's shallow water table depth and discharge excess water away from the agricultural field to a local surface water point. The

goal is to collect excess water from the soil profile into drainage pipes via the perforations at the times when the depth to the water table is lower than the distance from the surface to the drains. A subsurface drainage system is expected to provide trouble-free service for several years as long as the amount of soil cover required over the drains and the slope of the land with other essential topographic information are taken into consideration carefully before installation.

2.2 Nitrogen Transformations and Denitrification

Nitrogen is one of the primary nutrients associated with terrestrial and aquatic ecosystems and 79.1% of the earth's atmosphere composed of nitrogen gas (N_2). In many ecosystems, nitrogen is a scare resource because of its limited accessibility to most organisms when it exists in the form of nitrogen gas. Reactive nitrogen (Nr) term represents all biologically active forms of nitrogen that has a cascading impact on the environment and human-beings. Reactive nitrogen species include following: inorganic reduced forms (e.g. ammonia [NH_3] and ammonium [NH_4^+]), inorganic oxidized forms of N (e.g. nitrogen oxide [NO_x], nitric acid [HNO_3], nitrous oxide [N_2O] and nitrate [NO_3^-]) and organic nitrogen compounds. The migration of N species among the soil, water and atmosphere characterize the nitrogen cycle on a global scale. In terms of controlling biological activity in the soil, nitrogen is the most significant element just after carbon. The soil has its own internal nitrogen cycle that interacts with global processes result in nitrogen transformations to maintain the balance at numerous points. Nitrogen undergoes numerous different forms in an ecosystem because of the fact that the oxidation states of N enable transformation processes to take place. The valance state of the nitrogen varies from

+5 (electron-poor) to -3 (electron-rich) in its many combined transformations, as shown in Table 2.1.

Table 2.1: Forms of reactive nitrogen (Nr), formula, valence, and general chemical/physical state (Follett et al., 2010)

Ion or molecule	Formula	Valence of Nr	General State
Nitrate	NO_3^-	+5	Ion, highly soluble in water
Nitrogen dioxide	NO_2	+4	Gaseous
Nitrite	NO_2^-	+3	Ion, highly soluble in water
Nitric oxide	NO	+2	Gaseous
Nitrous oxide	N_2O	+1	Gaseous
Elemental N	N_2	0	Inert gas (nonreactive N)
Hydroxylamine	NH_2OH	-1	Liquid (>8°C)
Hydrazine	N_2H_4	-2	Oily liquid/white crystal
Ammonia	NH_3	-3	Gaseous
Ammonium	NH_4^+	-3	Ion, highly soluble in water

The dominance of any nitrogen compound present is subject to the environmental conditions of the aquatic ecosystem, particularly temperature, oxygen and microorganism activity coupled with the mineralization rates of labile organic nitrogen (Lee et al., 2006). Furthermore, the speciation balance can be controlled by seasonal alterations regardless of the total nitrogen concentration exist in the system (Burt et al., 1993).

In soil-water systems, nitrogen species can exist as ammonium-nitrogen (NH_4-N), nitrite-nitrogen (NO_2-N), nitrate-nitrogen (NO_3^--N), organic nitrogen and nitrogen gas. It is reported by the U.S. Geological Survey (USGS) that the usage of nitrogen-based fertilizer increased by almost 800% between 1960 and 2000 with rice, maize, and wheat corresponding to about half of fertilizer use, currently (USGS, 2015). The nitrogen

fertilizer use efficiency ordinarily drops below 40 percent, meaning that a vast majority of applied fertilizer is either washed out of the root zone or released to the atmosphere as N_2 before assimilating into biomass. The reactive nitrogen uptake through the roots of a plant from the soil typically occurs in the form of NO_3^- or NH_4^+ ions.

Worldwide, the usage of ammonium-based fertilizer stands for approximately 90% of the total, in which NH_4^+ can be converted into highly mobile NO_3^- that represents the stable end-product of the nitrification process. NO_3^- plays a critical role in primarily production and species diversity in aquatic and terrestrial habitats since it is the most commonly formed bioavailable nitrogen species (Mueller & Spahr, 2006). The influence of anthropogenic activities on N transformations, often causing high loads of NO_3^- in groundwater and surface water bodies (Rabalais et al., 2009). Nitrogen fertilizer and animal waste has been identified as major contributors to NO_3^- contamination in agricultural watersheds (Wieben et al., 2013). As NO_3^- quite soluble form of nitrogen in water and vulnerable to being removed from the unsaturated zone through water fluxes, the amount of NO_3^- exist in root zone beneath the fertilized agricultural sites is often proportional to precipitation and flow rate (Bakhsh et al., 2007; Cambardella et al., 1999).

Denitrification is the central process of the nitrogen cycle with respect to the subsurface groundwater environment and includes the conversion of soil NO_3^- back to nitrogen gas through a chain of microbial reductions (Knowles, 1982). While dinitrogen gas is the ultimate final product of the complete denitrification, other nitrogen gas species can be generated in one of the intermediate steps stated below.

$$NO_3^- \rightarrow NO_2^- \rightarrow NO \rightarrow N_2O \rightarrow N_2 \quad (2.1)$$

Each step enacted by specific enzymes that are in charge of the production of intermediate products mentioned in equation 2.1. These individual enzymes are called nitrate reductase (*nar*), nitrite reductase (*nir*), nitric oxide reductase (*nor*), and nitrous oxide reductase (*nos*) respectively. Each denitrification enzyme can be induced, principally in response to dissolved oxygen (DO) concentration and substrate C availability (Robertson & Groffman, 2015). There is a certain time interval between the production of a denitrification intermediate substrate and its consumption via the subsequent enzyme since enzyme induction proceeds sequentially and substrate dependent (Robertson & Groffman, 2015). Although denitrification process is expected to end with dinitrogen gas, the stable end product, the reaction can also produce NO_2 that is significantly more toxic than NO_3^- and N_2O, one of the primary greenhouse gases in the Earth's atmosphere. Under the conditions in which DO concentration in solution is quite low, N_2 is expected to be the final product; but, more intermediate or variable DO levels may arrest denitrification with the formation of NO_x (Brady and Weil, 2002). Additionally, low pH or quite high levels of nitrate stop the reaction at the N_2O stage (Rivett et al., 2008). The complete denitrification reaction relating NO_3^- and organic matter forms N_2, carbon dioxide (CO_2), and bicarbonate (HCO_3) if organic carbon is the electron donor.

$$5CH_2O + 4NO_3^- \rightarrow 2N_2 + HCO_3^- + CO_2 + 3H_2O \quad (2.2)$$

Based on the specified stoichiometry of denitrification reaction above, 1.25 moles of

dissolved organic carbon (DOC) are capable of reducing each mole of NO_3^- to N_2 if DO level in the solution is low enough not to inhibit the process.

Denitrification reaction is considered to be a significant part of the N cycle wherever O_2 concentrations become limiting. It is because of the fact that O_2 is the most thermodynamically favorable electron acceptor for oxidation of organic carbon in the saturated zone. In order for denitrification process to proceed efficiently, available O_2 concentration is supposed to be lower than 2 mg/L (Stenger et al., 2013). However, although denitrification occurs preferably under anoxic conditions, NO_3^- attenuation can take place through simultaneous heterotrophic nitrification and aerobic denitrification as well (Robertson et al., 1989). Bacteria in the saturated environment have a tendency to oxidize organic compounds or inorganic species (*e.g.* FeS_2, Fe^{2+}, Mn^{2+}) in order to generate cellular energy (Rivett et al., 2008). While denitrification can be performed by autotrophic denitrifiers as well, most of denitrifying facultative bacteria are known to be heterotrophic (Korom, 1992). A broad array of heterotrophic bacteria requires reduced carbon as the electron donor to denitrify during respiration. The main factor limiting denitrification rates is often found to be the deficiency of available organic carbon to supply energy to heterotrophic micro-organisms (Devito et al., 2000; Jacinthe et al., 1998; Pabich et al., 2001).

2.3 Denitrifying Bioreactors

Denitrification bioreactors are a relatively emerging management technology for NO_3^- removal from subsurface agricultural drainage water before it enters local water

bodies. The Environmental Protection Agency (EPA) has adopted 10mg/L standard as the maximum allowed concentration level (MCL) for NO_3-N and 1mg/L for NO_2-N for public water systems. Thus, nitrate concentrations higher than the MCL for NO_3^- in drainage waters ought to be considered as a potential threat to biodiversity of aquatic environments and warm-blooded animals. Typical NO_3^- concentrations detected in drainage waters without a treatment system vary from 10 to 35 mg/L (Schipper et al., 2010). NO_3^- mass removal rates for denitrification beds incorporating wood, are supposed to be in the range of 2 to 22 g NO_3^- removed per m^3 reactor volume per day if they are operated with appropriate field settings (Schipper et al., 2010).

Denitrification bioreactors were acknowledged as a new USDA NRCS national conversation practice standard (no. 605) published in September of 2015. Since these systems are federally approved, funding assistance provided by NRCS's Conservation Innovation Grants program for the construction of bioreactors has been available in line with the standard stated above. On the basis of drainage treatment, the most effective best management practices have been bioreactors and wetlands since both options can provide high percent load reduction (40% average) (Havill et al., 2017). On the other hand, areal NO_3^- removal rates for bioreactors is expected to be at least an order of magnitude higher than the ones achieved by wetlands (van Driel et al., 2006; Robertson & Merkley, 2009). Among other assessed agricultural practices include wetlands, buffers, and controlled drainage; denitrifying bioreactors were also defined as the most cost-effective edge-of-field application to remove nitrate from tile drainage on a dollar per pound basis (0.92 $/lb) (Hoover et al., 2017).

A denitrifying bioreactor is basically a trench excavated into the ground constructed at the edge of a tile system, thus it not necessary to take any portion of the agricultural site out of production. The trench is filled with a labile carbonaceous material to enable heterotrophic denitrifying bacteria to utilize dissolved carbon as electron donor through denitrification process. To date, woodchips have been utilized as fill substrate predominantly in order to intercept and decontaminate agricultural waters, leading to the terminology "woodchip bioreactor" that has been used to refer a denitrification bioreactor (Hoover et al., 2017). Denitrifying microbial populations, also known as nitrate-reducing bacteria (NRB), respire NO_3^- and convert it to inert N_2 under anaerobic conditions in the bioreactor chamber. Appleford et al. (2008) utilized denitrifying enzyme assays (DEA) to identify the types of microorganisms contributing to denitrification in subsurface bioreactors. They concluded that bacterial populations mediate denitrification process primarily while fungi enhance the overall performance of the reaction by releasing organic substrate molecules to bacteria from the woodchips. DEA analyses through the same study, furthermore, indicate that denitrification process can occur both in the aqueous phase and on the surface of the carbon substrate.

Carbon-based denitrification beds to treat tile drainage water have been researched for more than 20 years. Blowes et al. (1994) pioneered the usage of organic carbon materials (tree bark, wood chips, and leaf compost) to treat NO_3^- contamination from a farm-field runoff. The nitrate removal rate of the in-line bioreactor receiving drainage water containing nitrate contamination of 3-6 mg/L was sufficiently rapid to keep effluent NO_3^- concentrations below 0.02 mg/L throughout the variations in residence times. Several researchers have examined the performance of drainage denitrification bioreactors since

Table 2.2: Overview of selected field scale studies involving treatment of agricultural run-off through denitrification bioreactors

Reference	Site	Fill Material	Influent Nitrate Concentration	Percent Removal Rate of Nitrate
(Blowes et al., 1994)	Ontorio, Canada	Tree bark, wood chips and leaf compost	3 - 6 mg/L	Approximately 100%
(van Driel et al., 2006)	Southern Ontario, Canada	Fine and coarse wood particles	11.8 mg/L (cornfield site) 3.2 mg/L (golf course site)	33% (cornfield site) 53% (golf course site)
(Jaynes et al., 2008)	Central Iowa	Woodchips	19.1 to 25.3 mg/L	≥ 55%
(Robertson & Merkley, 2009)	Southern Ontario, Canada	Woodchips	4.8 mg/L	78%
(Moorman et al., 2010)	Northwest of Ames, IA	Woodchips	20 to 25 mg/L	≥ 50%
(Chun et al., 2010)	Decatur, IL	Woodchips	NA	47% load
(Verma et al., 2010)	DeLand, Illinois	Woodchips	3 to 15 mg/L (Performance Curves)	42% - 48% load
(Verma et al., 2010)	Decatur, Illinois (west)	Woodchips	5 to 23 mg/L (Performance Curves)	81% - 98% load
(Verma et al., 2010)	Decatur, Illinois (east)	Woodchips	4 to 15 mg/L (Performance Curves)	54% load
(Woli et al., 2010)	DeLand, East-Central Illinois	Woodchips	2.8 to 18.9 mg/L	33%
(Christianson et al., 2012)	Pekin, Iowa	Mixture of gravel and woodchips (60% woodchips by volume)	1.2 to 7.8 mg/L (annual mean)	22% - 74% load
(Christianson et al., 2012)	Northeast Iowa	Woodchips (100%)	9.0 to 11.3 mg/L (annual mean)	11% - 13% load
(Christianson et al., 2012)	Greene County, Iowa	Mixture of shredded material and chips	7.4 to 12.8 mg/L (annual mean)	27% - 33% load
(Christianson et al., 2012)	Hamilton County, Iowa	Woodchips (100%)	7.03 to 13.11 mg/L(annual mean)	49% - 57% load
(Hassanpour et al., 2017)	Tompkins County, NY	Mixture of biochar and woodchips (90% woodchips)	9.3 mg/L	42% - 55%
(Hassanpour et al., 2017)	Chemung County, NY	Mixture of biochar and woodchips (90% woodchips)	6.2 mg/L	66% - 68%
(Hassanpour et al., 2017)	Steuben County, NY	Mixture of biochar and woodchips (98% woodchips)	16.6 to 18.4 mg/L	58%-62%

NA – Not Available

the first study mentioned above. Selected field-scale drainage treatment studies are summarized in Table 2.2.

2.3.1 Performance Controlling Parameters of Denitrifying Bioreactors

2.3.1.1 Denitrification Kinetics and Influent Nitrate Concentration

The main chemical reaction provides NO_3^- removal in bioreactors is found to be microbial heterotrophic denitrification (Warneke, Schipper, Matiasek, et al., 2011). According to past analysis of field-scale and lab column studies, the chemical mechanism of denitrification process can fit both zero and first order kinetics depends upon the NO_3^- concentration of tile drainage effluent. Some previous researchers have reported that denitrification kinetics at influent NO_3^- concentrations greater than 1mg/L are zero order (*i.e.* independent of concentration), suggesting that removal rate is controlled by another parameter (presumably the release rate of degradable C from the carbonaceous media) (Korom et al., 2005; P. W. van Driel et al., 2006; Warneke, Schipper, Matiasek, et al., 2011). While the effect of fluctuating NO_3^- inputs on denitrification rate is limited since denitrifying microbial population can survive even though influent nitrate concentrations are very low, fluctuations in NO_3^- input can lead to the depletion of available carbon steadily (Schipper & Vukovic, 1998). A transition to first-order kinetics can take place at lower concentrations where denitrification rate is strongly proportional to daily average NO_3^- concentrations, but in most settings, denitrification process in bioreactor is likely to obey zero-order kinetics (Schipper et al., 2010). This theory was verified in a series of column experiments with different aged woodchip media (0 to 7 years) which were

conducted to estimate if there is a positive correlation between increasing inlet NO_3^- concentrations of from 3.1 to 49 mg/L and nitrate removal rate (Robertson, 2010). While it is concluded in the same study that influent NO_3^- is not the rate-limiting substrate since NO_3^- mass removal rates stayed relatively constant over the concentration range, Addy et al, (2016) reported lower NO_3^- mass removal rate at lower concentrations, which may depict why N input levels are also required to be taken into consideration for bioreactor design.

As an enzyme catalyzed reaction, denitrification, is assumed to follow the general equation of the Michaelis - Menten kinetics which is utilized to describe denitrification process in the soil environment (Laudone et al., 2011). The denitrification rate with respect to nitrate as the substrate can be estimated by this equation.

$$r_{NO_3} = \frac{V_{max} C_{NO_3}}{K_M + C_{NO_3}} \tag{2.3}$$

In equation 2.3 r_{NO_3} represents the hourly nitrate attenuation rate in mg L^{-1}, V_{max} is the maximum nitrate removal rate achieved in the system (mg L^{-1} h^{-1}), the Michaelis constant, K_M (sometimes represented as K_S instead) (mg nitrate L^{-1}), is the NO_3^- concentration at which reaction rate is equal to half of maximum removal rate, and C_{NO_3} is the influent NO_3^- concentration (mg L^{-1}). It is ought to be highlighted that C_{NO_3} is typically assumed to represent the total NO_3^- concentration exist in the system of the interest – which stands for, in fact, the free NO_3^- concentration in the domain. This assumption is called free ligand

approximation, and valid for the systems in which the rate constant is well above the total enzyme concentration present in the system.

As stated before, if NO_3^- concentrations exceed the microbial capacity for attenuation, NO_3^- removal is likely to fit zero-order kinetics. In this cases, the Michaelis-Menten equation can be simplified since rate constant of the denitrification reaction is quite lower than initial nitrate concentration.

$$r_{NO_3} \cong V_{max} \tag{2.4}$$

In addition to microbial denitrifier biomass, carbon substrate availability can be considered as another limitation to NO_3^- removal rate at these higher initial nitrate concentrations. First order representation of the Michaelis-Menten model is required to be applied at low substrate concentrations where increasing denitrification rates are correlated with ascending inflow nitrate.

$$r_{NO_3} \cong \frac{V_{max} C_{NO_3}}{K_M} \tag{2.5}$$

Taking the reciprocal of both sides of Eq. (2.3) derives the Lineweaver - Burk (also known as the double - reciprocal) equation that is utilized to obtain K_M and V_{max} values accurately.

$$\frac{1}{r_{NO_3}} = \frac{K_M}{V_{max}} \frac{1}{[C_{NO_3}]} + \frac{1}{V_{max}} \quad (2.6)$$

The inverse of the denitrification rate is graphed as a function of the inverse of the influent NO_3^- concentration to yield a linear line with a slope of K_M/V_{max} and y-intercept of $1/V_{max}$.

2.3.1.2 Hydraulic Retention Time (HRT)

Hydraulic retention time (HRT) is one of most significant design parameters not only for bioreactors but also other engineering-based solutions which are designed to prevent water flowing quite fast through a media that can lower nitrate attenuation performance of the system. Designers of the denitrifications beds ought to optimize the system based on predicted flow rates to ensure sufficient time required for desired nitrate removal rates (Addy et al., 2016). Hydraulic retention times are expected to alter throughout the year due to the high seasonal variability in the flow rates of drainage effluents entering bioreactors. In order to manage this uncertainty, most of the proposed denitrifying bed systems incorporate upstream and downstream hydraulic control components (also known as control structures) which enable researchers to adjust retention times (Figure 2.2). The inline water level control structure is used to divert the flow into the bioreactor and control how much drainage water can bypass the bioreactor and discharge directly to a ditch or surface water body. The outflow control structure with a weir is utilized to adjust the water level within the bioreactor via setting the level of the weir. Thus, the outflow control component is responsible for controlling the retention time in line with the drainage flow intensity and duration. For instance, this control structure should be lowered to ensure the

HRT will not be quite high during the periods when no or weak flows are observed (*e.g.* late summer). Likewise, when the bioreactor is receiving relatively higher amount of flows (*e.g.* spring), it is ought to be raised to maintain an adequate retention time (Christianson, 2011). Based on the general design criteria for denitrifying bioreactors recommended by the USDA natural resources conversation practice, edge-of-field denitrification

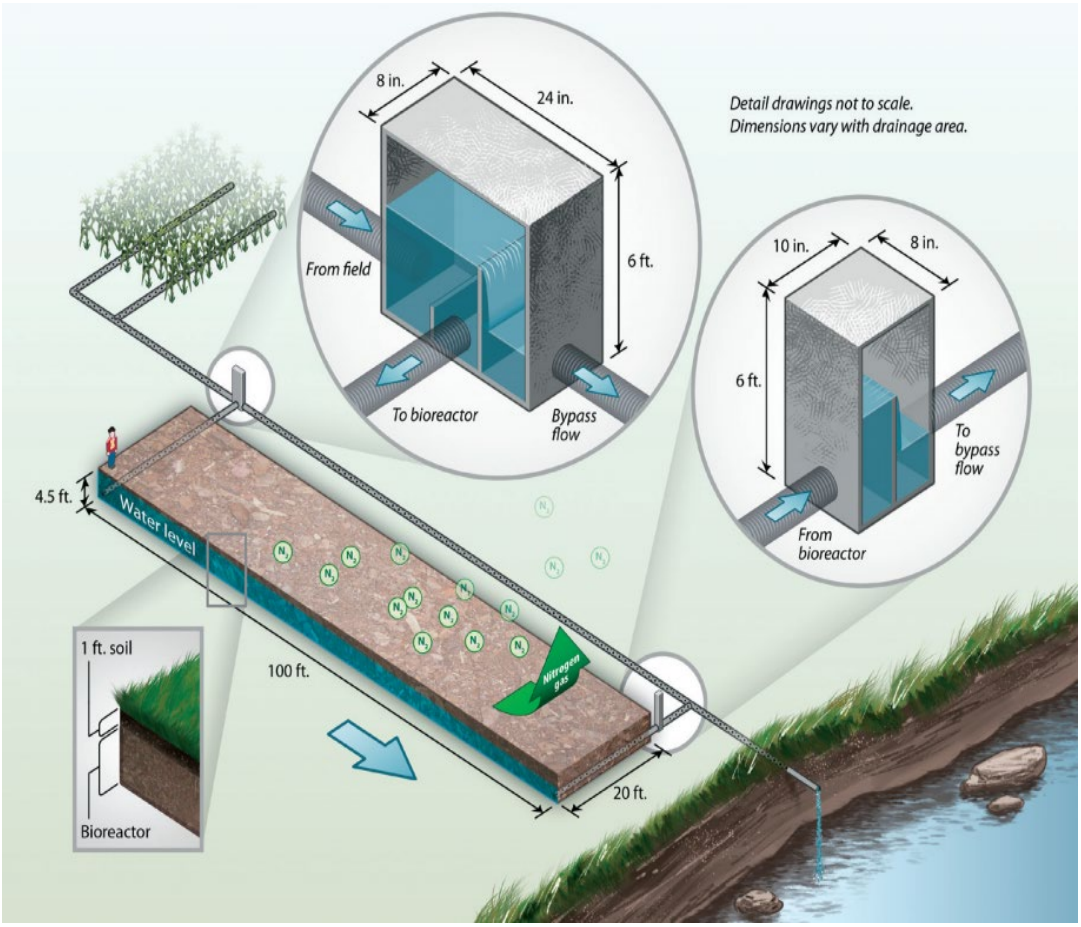

Figure 2.2: Descriptive illustration of a denitrification bioreactor with control structures (Christianson & Helmers, 2011)

bioreactors typically requires lower HRTs during peak flow conditions. Designing a denitrification bioreactor according to predicted total amount of drainage water from farm-

field would call for quite high installation costs. The current NRCS conservation practice standard recommends treating at least 15 percent of the peak flow from drainage effluent (NRCS, 2015). Further, it is suggested in the same standard that bioreactor HRTs are supposed design for a minimum of 3 hours at the peak flow capacity. Quite low retention times can be observed during high flow situations and it may result in limited NO_3^- removal which is attributed to insufficient reaction time for denitrification to proceed efficiently (Cooke et al., 2001). Prolonged retention time, on the other hand, is likely to result in complete NO_3^- removal, but also creating suitable conditions for undesirable reactions like sulfate reduction or the methylation of mercury (Blowes et al., 1994; Shih et al., 2011).

HRT of a field-scale bioreactor is expected to be highly variable throughout the year due to the fluctuation in drainage flow rates. Alteration in retention times is often correlated with bioreactor pore volume and specific drainage discharge. HRT (in hours) can be calculated as

$$HRT = \frac{A\rho d}{Q} \tag{2.7}$$

where A is the surface area of the bioreactor (m^2), Q is the hourly drainage discharge rate ($m^3\ h^{-1}$) d is the active height of water in the bioreactor (m) and ρ is the effective porosity of the carbonaceous fill media (Christianson et al., 2011). Effective porosity (also known as drainable porosity or specific yield) corresponds to the portion of the total porosity contributing to fluid flow through carbon media (Ghane et al., 2015). Unlike the effective porosity, total porosity is estimated by considering pore-bound water as well which is

typically obtained by drying material of interest. Total porosity values of attributed to woodchip media was calculated as 0.85 and 0.89 (Ghane et al., 2015; Hoover et al., 2016) while reported *in-situ* values typically range from 0.60 - 0.79 (Chun et al., 2010; Hoover et al., 2017; Woli et al., 2010). A standard porosity value of 0.70 for field bioreactor design has also been stated in the literature (Addy et al., 2016; van Driel et al., 2006). As can be predicted, porosities of larger sized fill media (*e.g.* woodchips) was greater than the ones estimated for carbon media with smaller grain size like sawdust - and lower porosity will contribute to shorter HRTs during intense rainfall events in particular (Schipper et al., 2010). Ima and Mann (2007) have also concluded that woodchip porosity is inversely proportional to increased moisture content.

The potential of carbon-based bioreactors in terms of NO_3^- removal rates with various retention times has been extensively studied at both field and laboratory scale. At most of field scale studies, it is concluded that longer HRTs result in increased NO_3^- removal efficiency (van Driel et al., 2006; Robertson, 2010; Woli et al., 2010). Hassanpour et al. (2017) were monitored six denitrifying bioreactors that were installed on farms to find the relationship between NO_3^- removal efficiency and HRT for the events with varying drainage water temperatures. They defined a critical HRT at which complete NO_3^- removal ensued and it was longer for the temperatures below 16°C. Below this critical retention time, they found that removal efficiency linearly correlated with ascending HRTs. Hoover et al. (2016) studied a woodchip bioreactor at the lab scale and they reported NO_3^- removal efficiency from 8 to 55 (percent removal) with increased retention times. On the other hand, NO_3^- mass removal rates (load reduction) which is expressed in g nitrate $m^{-3}hour^{-1}$

did not follow the same trend, and almost remained constant as HRT increased from 1.7 to 21.2 h in the same study. Therefore, it may suggest that relatively equivalent loads of NO_3^- will be reduced through a given time scale regardless of retention time. In the top layer of the denitrification bioreactors which is unsaturated for most of the case, suitable conditions facilitating nitrification of organic nitrogen can ensue during intense or transient flow events. Thus, even negative percent removal efficiency can be observed within a narrow range of HRT (van Verseveld et al., 2009).

2.3.1.3 Temperature

Temperature is another critical parameter that needs to be considered in the design of the carbon-based denitrification process. As a biologically mediated reaction, denitrification in a bioreactor is expected to be dependent on drainage water temperature. Generally speaking, temperature change can affect microbiological processes in two ways. It can either accelerate the rates of processes without modifying fundamental behaviors of microbial communities or restructure the microorganisms present in the system which could stimulate processes that were previously insignificant (Schimel & Gulledge, 1998).

The optimum temperature range for denitrification to proceed is known to be from 25 to 35°C. The reduced biological activity thanks to a decrease in temperature is important particularly for biological denitrification where the drainage water temperature drops to below 6 °C during the winter months (Addy et al., 2016). Alterations in denitrification rate due to seasonal temperature variations may be masked on account of fluctuations in the rate of DOC flux (Rivett et al., 2008). The typical denitrification beds incorporating wood media are considered to be effective in NO_3^- removal when they are

operated in the temperature range of from 2 to 20 °C (Schipper et al., 2010). Increasing NO_3^- removal rates can be correlated with the temperature coefficient, Q_{10}, which refers the change in reaction rate of biological or chemical process as a consequence of raising the temperature by 10°C. The Q_{10} is calculated as

$$Q_{10} = \left(\frac{R_2}{R_1}\right)^{\frac{10}{T_2 - T_1}} \quad (2.8)$$

where, R is the denitrification rate (g N m^{-3} day^{-1}) and T is the temperature in Celsius degrees or kelvins. In the equation 2.8, Q_{10} factor is a unitless quantity which varied in the range between 1.2 and 4.7 for denitrification bioreactor studies (Addy et al., 2016; David et al., 2016; Hoover et al., 2016; van Driel et al., 2006; Schmidt & Clark, 2013; Warneke et al., 2011). Warneke et al. (2011) found that in addition to temperature, carbon availability is also a limiting factor to denitrification, therefore, determining temperature coefficient may require to consider the influence of carbon fill material as well. At relatively low temperatures, on the other hand, DO concentrations can be higher which is likely to inhibit denitrification rates, illustrating that reduced NO_3^- removal rates as a consequence of higher DO concentrations, and a potential decrease in the activity of denitrifying microbial communities can be influential factors in Q_{10} determination at lower temperatures (Hoover et al., 2016). It has been hypothesized in most of the both field and pilot scale bioreactor studies that denitrification rate doubles every 10°C increase in temperature (Q_{10} = 2.0), supporting the assumption that the temperature sensitivity of denitrification process in the bioreactor can be described by the Arrhenius equation. While this function can be utilized

to determine exponentially increased denitrification rates within a certain temperature range, it fails to predict an optimum temperature (T_{opt}) above which the denitrification rate remains almost stable or even decline. Temperature effect on denitrification rate will be discussed in more detail in the methodology and performance modeling section.

Addy et al. (2016) have reviewed 26 published studies related to the denitrification bioreactors with a broad range of environmental and design conditions. The authors concluded that denitrification beds operated with temperatures lower than 6°C had lower NO_3-N removal rates than the ones at intermediate temperatures from 6 to 16.9°C and those at temperatures higher than upper limit of intermediate temperature category. Further, they did not state significant difference in nitrate removal rates of the denitrification beds operated within intermediate temperatures mentioned below and temperatures higher than 16.9°C. This finding may be considered as an evidence for the uncertainty of the response of denitrification process in bioreactors to changing temperature beyond T_{opt}.

2.3.1.4 Carbon Media

Organic carbon source is oxidized via facultative anaerobic heterotrophs to supply their energy in the process where NO_3^- is utilized as energetically favorable electron acceptor. In addition to act as an electron donor for denitrification process, the presence of organic carbon is critical to provide an anoxic environment in the bioreactor since aerobic bacteria reduce DO concentrations through oxidation of organic compounds (Rivett et al., 2008; Schipper et al., 2010). Products of the process of breaking down hard or soft wood cellulose and lignin into the bioavailable carbon will be in the forms of amino acids,

carbohydrate and other simple organic compounds (Zou et al., 2005). Thus, DOC concentrations detected in a denitrification bioreactor can be taken into account as an indicator of the bioavailable carbon (Hoover et al., 2017). Since the decomposing organic C generates substantial amount of DOC in the bioreactors, concentrations measured in the effluent are typically greater than those in drainage water. Hoover et al. (2017) reported that in the cases when DOC concentrations detected in the inlet at most two times lower than the ones at the outlet, nitrate removal efficiency decreased dramatically. The degradation of organic compounds is expected to increase with increasing temperatures which may result in excessive quantity of DOC than can even exceed the amount required for complete denitrification (Paré et al., 2006).

The physical and chemical properties of the carbon media are known to be significant to maintain a consistent reduction in nitrate concentration over long periods. C:N ratio that refers foundational C bioavailability of the media is inherently correlated with NO_3^- attenuation and potential degradation rates. The surface area of the carbonaceous media may have an influence on denitrification rates as a consequence of increased microbial activity and extracellular enzyme exposure (Schmidt & Clark, 2013). In order to examine the impact of the surface area, Robertson et al. (2000) experimented carbon media of differing grain sizes and they found no consistent or considerably influence on denitrification rates. This study may demonstrate that grain size ought not to be considered as a major determinant of the surface area because of its interrelationship with effective porosity (Schmidt & Clark, 2013). Cameron & Schipper, (2010), on the other hand, reported a positive correlation between grain size and nitrate removal rates in the softwood treatments at 14°C, but there was not such a tendency stated for the experiments at 23.5°C.

Since the coarser sized woodchip media is supposed have higher porosity and provides longer HRTs, they suggest that increased removal rates may be positively correlated with the grain size. The mean particle diameter distribution reported in the of woodchip bioreactors studies have been in the range from 6 to 25 mm (Christianson et al., 2010; Chun et al., 2010; Hassanpour et al., 2017; Woli et al., 2010). The hydraulic conductivity (K) of the carbon media is another significant indicator describing the ease at which drainage water flows through pore space in the presence of a hydraulic gradient. This parameter is dependent not only the effective porosity of the carbon media but also -and primarily- on the sizes of conducting pores. Over a long period of time, K value can decline as a consequence of narrowing pore size due to microbial growth and/or wood degradation - induced compaction (Schmidt & Clark, 2013). The hydraulic conductivities for woody-based fill media in place vary from approximately 0.28 cm/sec for fine grained sawdust to 11.6 cm/sec for woodchips (Cameron & Schipper, 2010; van Driel et al., 2006; Robertson et al., 2005). In a 22-month wood-only bioreactor experiment, a marked reduction in the value of K in coarser grained media (>10mm) was reported (Cameron & Schipper, 2010). This considerable decline (23-56%) was attributed to the impact of alterations in media particle geometry and inclination for settling of the carbon subtract particles on their flat surface. Contrary to the findings of this laboratory trial, there was no consistent K trend with increasing size of different wood types in another bioreactor experiment lasting 246 days (Schmidt & Clark, 2013).

To date, woodchip media have been the most prevalent fill material for denitrification bioreactors, because of its accessibility, cost, relatively slow decomposability under anaerobic conditions, appropriate hydraulic properties and

consistent NO_3^- removal rates for long periods after the release of labile carbon in the early stages of start-up period. (Blowes et al., 1994; Christianson et al., 2012; Chun et al., 2010; Schipper et al., 2010; Warneke et al., 2011). In addition, it is not required to replace woodchip-based materials since the leaching of organic carbon from them does not occur rapidly, even though the duration of NO_3^- removal efficiency is subject to the duration of the carbon supply to the denitrifying bacteria populations (Moorman et al., 2010). In addition to wood particle media (woodchips/sawdust), a great variety of carbonaceous substrates including wheat straw, leaf compost, rise husk, cotton burr, corn stalks and maize cobs have been successfully trialed especially in column studies in order to establish the most efficient fill material for heterotrophic denitrification (Cameron & Schipper, 2010; Della Rocca et al., 2005; Gibert et al., 2008; Saliling et al., 2007; Soares & Abeliovich, 1998). The considerable high NO_3^- removal rates of some carbon fill materials (e.g. wheat straw, rise husks, maize cobs) in 0.2 m^3 barrels have observed in a long term study conducted by Cameron & Schipper (2010). For instance, maize cobs provided 3-6.5 times higher NO_3^- removal rates than those reached with barrels filled with wood media. This significant difference in removal rates was attributed to great amounts of organic carbon leaching in the start-up phase of the denitrification trials, and were not sustainable throughout a long period of time (Cameron & Schipper, 2010). In a laboratory denitrification study, different types of organic carbon rich media (lodge pole pine woodchips (LPW), lodge pole pine needles (LPN) and barley straw (BBS) and cardboard) were experimented in which percent NO_3^- removal efficiency ranged from 67% for LPW to 95% for cardboard when potential adverse effects of the bioreactors were also taken into

account (Healy et al., 2012). In order to enhance denitrification rate and minimize adverse effects include TOC decomposition, dissolved N_2O release and substantial consumption rate of organic C, an appropriate combination of woodchips and maize cobs were recommended in an experimental study (Warneke, et al., 2011). Similarly, the addition of soybean oil to woodchips contributed to higher NO_3^- removal rates compared to the trial with woodchips alone observed in another laboratory study (Greenan et al., 2006).

2.3.1.5 Effects of Other Physical Characteristics

In addition to the aforementioned most influential parameters on the rate at which NO_3^- attenuation occurs, some previous field and pilot scale studies indicated that pH, dissolved oxygen concentration and oxidation reduction potential (ORP) are also required to be taken into consideration as site-specific parameters to predict performance of the bioreactor accurately.

The direct pH response to overall denitrification rates is known to be depend on the composition/structure of the functional denitrifying microbial populations (Dörsch et al., 2012) or the nature of the carbon media (Drtil et al., 1998). The preferred pH range for heterotrophic denitrification is typically between 5.5 and 8.0 (Rust et al., 2000), but the optimal pH for denitrification process cannot be specified as this value can vary site by site due to the influences resulted from acclimation and adaptation on microbial environment (Rivett et al., 2008). The pH of the drainage water in the bioreactor is expected to increase several units during denitrification since NO_3^- is consumed while HCO_3 and CO_2 are released at the same time (Eq 2.2), also pH increase can occur under the conditions in

which the formation rate of OH^- exceeds that of CO_2 (Rivett et al., 2008). Slightly decreased pH values from influent to effluent of denitrification beds have been reported in some studies as well (van Driel et al., 2006; Robertson et al., 2005; Robertson & Merkley, 2009). The pH values lower than 5.0 can create a microbial ecosystem that has a tendency to inhibit the conversion of N_2O to N_2 (Knowles, 1982; Warneke, et al., 2011), and high pH values stimulate N_2O formation due to potential activation of N_2O reductase enzyme (Downie et al., 2009). Rust et al. (2000) quote that the denitrification chain is arrested at pH values higher than 8.3. Cameron & Schipper, (2010) found that the start-up outflow pH of the bioreactor treatment studies have ranged from 2.5 to 6.6 (hardwood = 2.5 and softwood = 4.3), and then it reached a pH value of 6.6 for each media type within the first 3 months. The lower initial NO_3^- removal rates observed in the hardwood experiments in comparison to those measured in the softwood trials were attributed to strongly acidic environments (Cameron & Schipper, 2010; Greenan et al., 2006).

Drainage water entering a denitrification bioreactor naturally comprise DO that has to be consumed initially as electron acceptor by aerobic microorganisms in the system. Because, the attenuation of NO_3^- is thermodynamically less favorable reaction than reduction of DO as mentioned before. To consider an aquatic ecosystem ideal for denitrification to proceed, DO concentrations are ought to be less than or equal to 1-2 mg/L (Rivett et al., 2008). The DO present at inhibitory levels within the denitrification bioreactor limits the action of the nitrite reductase enzyme in particular rather than nitrate reductase (Rivett et al., 2008). Under the conditions in which DO concentrations are in the range stated above, denitrifying bacteria convert N_2O to N_2 gas by utilizing O_2 in the N_2O, and when DO>2mg/L, microorganisms donate electron to O_2 molecule in place of N_2O

(Knowles, 1982). Until DO levels in the bioreactor fall below the threshold concentrations, labile organic carbon is utilized through aerobic respiration rather than denitrification. A substantial amount of organic carbon substrate is likely to be consumed if the bioreactor is operated with relatively insufficient hydraulic retention times (Robertson, 2010). In a study undertaken with a two year old woodchip bioreactor, it was found that a HRT of almost 1h is required to reduce DO concentrations to a level that allows denitrification process to occur (Schipper et al., 2010). Increasing concentrations of DO in the influent water have been correlated to relatively lower temperatures which in turn contributed to decreasing NO_3^- attenuation rates since DO reduction must take place before the onset of denitrification (Robertson & Merkley, 2009; Schipper et al., 2010; Shih et al., 2011). The effluent DO levels were found to be lower than 2.4 mg/L regardless of inlet DO concentration in a field-scale study (Christianson et al., 2012). Commonly observed effluent DO concentrations did not meet the national water quality criteria determined by USEPA, which requires to maintain a daily minimum DO concentration of 5.0 mg/L during spawning season to protect aquatic wildlife species. However, denitrification bioreactors often discharge into relatively small-scale streams or agricultural ditches that have high reaeration-rate coefficients in general (Melching & Flores, 1999). If bioreactors are taken advantage of intensively in a region consisting of agricultural sites, low outlet DO levels may be a cause of concern for the area of interest (Bell et al., 2015).

It may be required to monitor ORP within the bioreactor as another potential control variable for proper evaluation of denitrification process. Mo et al. (2005) reported that the ORP levels remained fairly stable in the range from -230 to -120 mV when complete denitrification was achieved in the system designed to remove NO_3^- from

groundwater. They also correlated increasing NO_3^- loading rates with higher ORP values which contributed to incomplete denitrification with residuals of NO_3^- in the system. The high ORP values can result in the accumulation of denitrification by-products due to decreased enzymatic activity (Knowles, 1982; Rivett et al., 2008). The ORP value in the bioreactor is expected to decrease during the denitrification reaction as a consequence of the decrease in the level of oxidants, and immediately returned to the initial level after NO_3^- was completely removed (Drtil et al., 1998; Song et al., 2003).

2.3.2 Potential Adverse Effects of Operating Denitrifying Bioreactors

2.3.2.1 Nitrous Oxide Emissions

Denitrification bioreactors may cause potentially harmful environmental issues while treating NO_3^- contamination and enhancing overall water quality of subsurface drainage systems. N_2O, one of the intermediate products of biological NO_3^- removal process, is produced before the formation of N_2 gas under favorable conditions (Eq 2.1). The release of N_2O into the atmosphere or surface water bodies in the dissolved form is a matter of concern since it is known that even a relatively small amount of N_2O can contribute to global warming, acid rains and ozone layer depletion in the upper atmosphere (310 times that of carbon dioxide). The N_2O emissions in the absence of complete denitrification were correlated to fluctuated DO levels, low pH values and high N loads into bioreactors (Healy et al., 2012; Brady and Weil, 2002; Rivett et al., 2008). The potential influence of different carbon substrates on the production rate of dissolved N_2O in the effluent was also evaluated in a 2.5-year experiment, and it is concluded that

bioreactors filled with wheat straw had the largest amount of N_2O in the outlet water which corresponded to 10% of the removed NO_3^- (Warneke et al., 2011). They also reported 7 times more dissolved N_2O on average at 27.1°C (when NO_3^- removal was the highest) compared to those at 16.8°C for the treatments with all carbon substrates. The N_2O flux from a denitrification bed with complete or near-complete NO_3^- removal is likely to be the lowest (Schipper et al., 2010). In a stream-bed bioreactor study, the measured dissolved N_2O was quite higher in the case with incomplete denitrification(10-35 μg N L^{-1}) in comparison to the period when complete nitrate removal occurred (0-5 μg N L^{-1}) (Elgood et al., 2010). In addition to the dissolved concentrations of N_2O, measured emission rates of N_2O per unit surface area along the length of denitrification beds have also been utilized to quantify this adverse effect in some studies (David et al., 2016; Ghane et al., 2015; Healy et al., 2012; Woli et al., 2010). An average N_2O surface emission of 0.12 μg N m^{-2} min^{-1} from a woodchip bioreactor was reported in a field-scale experiment (Ghane et al., 2015). Similarly, a very low percent of the removed NO_3^- in the form of N_2O (less than 1%) was observed in a recent study (David et al., 2016).

2.3.2.2 Sulfate Reduction

Facultative bacteria utilize the electron acceptors present in the drainage water sequentially in accordance with the redox potential of each possible reaction in which released organic carbon is oxidized. In general, microbes have a tendency to catalyze, and obtain energy from, the most energetically favorable reduction-oxidation reaction. Thermodynamically, denitrifying bacteria are likely to out-compete sulfate reducing

organisms for biologically available carbon, consequently reduction of the most sulfate may take place under the conditions that are favorable for the production of hydrogen sulfide gas (H_2S), a poisonous and corrosive gas. The aquatic environment that has an ORP value within the bioreactor falls below the lower limit of the range indicating complete denitrification will stimulate the conversion of sulfate to H_2S.

Sulfate is likely to exist in the drainage water, thus it is able to be a substitute for NO_3^- in the lack of it in order to oxidize C substrate (Moorman et al., 2010; Woli et al., 2010). The detection of rotten egg odor may indicate the presence of H_2S gas at the effluent of a bioreactor. Declined sulfate concentrations from inlet to outlet and the H_2S odor were noted in the presence of NO_3^- concentrations below 1mg/L (Elgood et al., 2010; Robertson, 2010). Prolonged retention times provide complete or nearly-complete denitrification before the onset of sulfate reduction. In experimental runs, the highest percent NO_3^- removal and formation of H_2S rates were attributed to longer retention times (Bell et al., 2015). Apart from the influence of HRT, the conversion of sulfate to H_2S gas was also correlated to high drainage water temperatures (Schmidt & Clark, 2013).

2.3.2.2 Production of Methyl Mercury

Strongly reducing conditions can result in the production of toxic methyl mercury (MeHg), a non-point source pollutant, from inorganic mercury through sulfate reducing bacteria. According to the World Health Organization (WHO), human or wildlife exposure to MeHg is known to cause a variety of health risks like neurological damage resulted from the consumption of MeHg-contaminated marine products. Shih et al. (2011) recommend

retaining NO_3^- levels greater than 0.5 ppm in the effluent in order to minimize the methylation of mercury. In addition to maintaining very low NO_3^- concentrations, Christianson & Helmers, (2011) also suggest adjusting the height of outflow stoplogs in line with the intensity of drainage flows to avoid MeHg production and sulfate reduction.

2.3.3 Longevity

The longevity of NO_3^- removal in denitrification bioreactor is mostly subject to the physical and hydraulic properties of carbon media. In terms of the leachate of carbon media, heterotrophic denitrification is not the only reaction of interest since undesirable processes like sulfate and/or DO reduction can also consume microbially available organic C in the system. The degradation rate of carbon substrate is known to be inhibited to some extent under consistently water saturated conditions because of the fact that a majority of microbes that are in charge of breaking down solid carbon cellulose and lignin call for aerobic conditions (Moorman et al., 2010; Schipper et al., 2010). The half-life expectancy of a bioreactor mostly operated with woodchips that were below water table was estimated to be 36.6 years with maintaining more than 80% of the initial C (Moorman et al., 2010). In the same study, they reported retained 25% of the background C mass after 8 year of operation for the woodchip decomposition under variable saturated conditions. Addy et al. (2016) illustrated that NO_3^- removal rates for <13 month old denitrification beds were significantly higher than those >13 month old. On the other hand, annual C content consumption of less than 2% through solely denitrification process was also reported (van Driel et al., 2006; Robertson & Merkley, 2009).

CHAPTER 3. METHODOLOGY AND PERFORMANCE MODELING

3.1 Site Description

The field-scale denitrification bioreactor evaluated in this study was previously installed at the Oregon State Experimental Dairy Farm in Corvallis, OR in September 2017 (Figure 3.1). It was constructed at the edge of a subsurface drainage system that is installed beneath an agricultural field to remove excess water from the soil profile through clay pipes. The 24-inch diameter drainage tiles that the system tapped into had been installed at a depth of approximately 4 ft. with a parallel spacing of 55 ft. The collected water is aimed to discharge into a local ditch which runs west to east through within the property. The bioreactor was built immediately adjacent to the west edge of the ditch with the dimensions 24 ft. long, 6 ft. in width, and installed to a depth of around 3.3 ft. below ground surface (Figure 3.2).

Figure 3.1 Approximate location of the bioreactor located in the OSU Dairy Farm

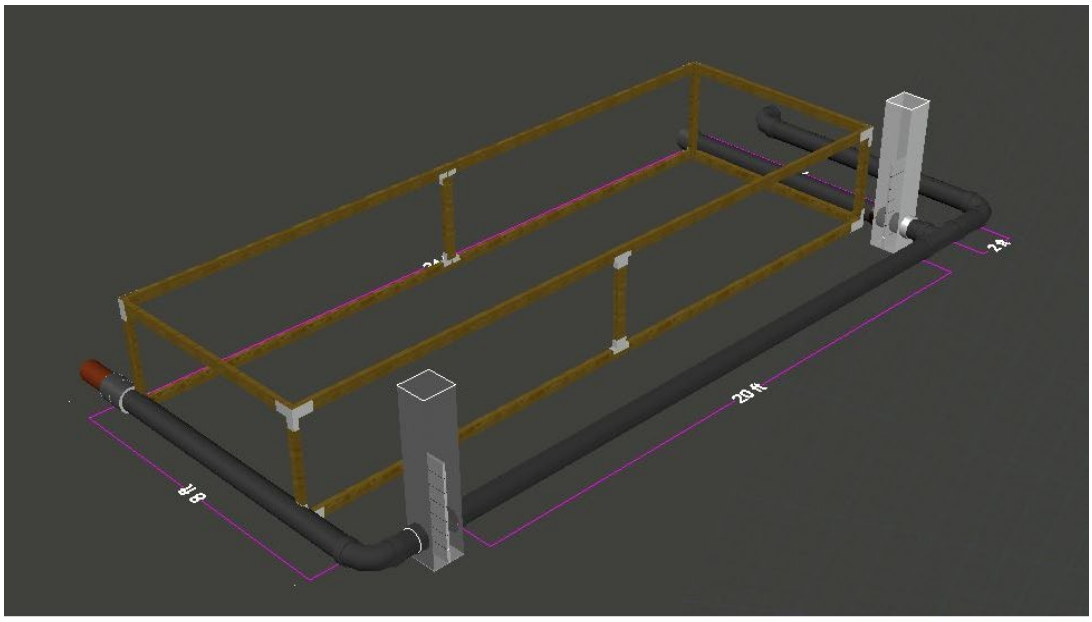

OSU Dairy Farm Upstream Bioreactor General Layout

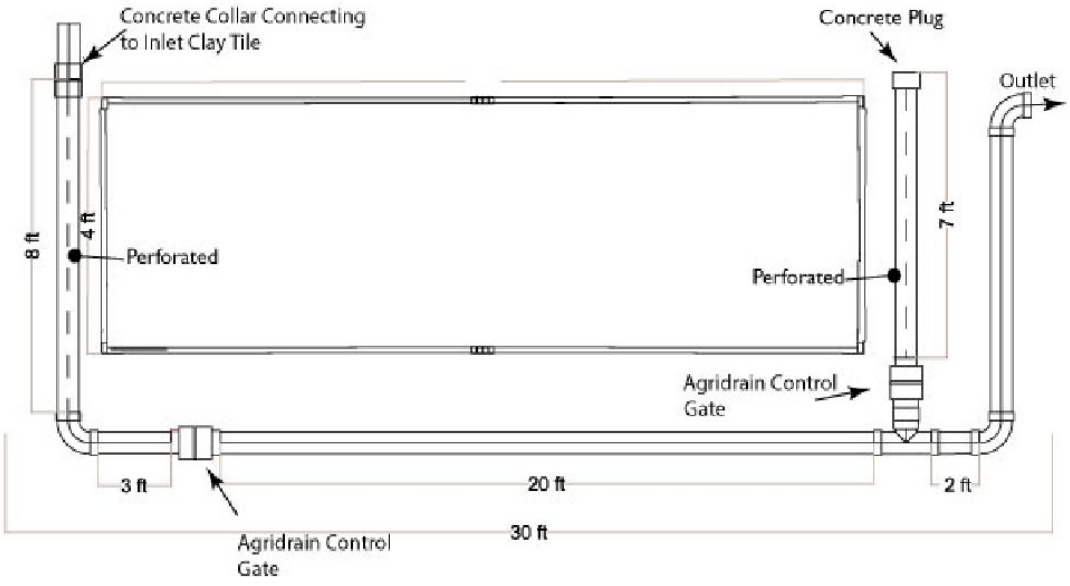

Figure 3.2: The schematic drawings of the full-scale woodchip denitrification bioreactor (Grohman, 2017)

As demonstrated in Figure 3.2 in detail, the bioreactor constructed to intercept drainage water from the site and have two AgriDrain control structures. The main drainage clay line from the field is connected to a 12-inch diameter perforated PVC pipe, then drainage water is laterally distributed along the entire width of the bed. An inflow control structure was installed near the upstream of the bioreactor to route untreated water directly into the ditch via 20-ft long by-pass line during high precipitation periods. The total active flow volume of the bioreactor is 475.2 ft^3, but it can be adjusted by raising or lowering stop logs present in the control structures. After infiltration stage in the bioreactor, water is collected through a 6-inch corrugated pipe leading to the outflow control component at the downstream end of the bioreactor. The collection manifold line is connected to the two-chamber outlet control structure that can be utilized to control hydraulic retention time and maintain the water level by adjusting the level of weir the inside when necessary.

The denitrification bed is a trench excavated 1 m below the ground surface and filled with coarse woodchips that have an approximate length in the range from 10 to 50 mm. The bioreactor was covered along the bottom and sides with clear, 0.25-mm-thick geotextile fabric material just before being mounded with top soil layer. The transparent geotextile liner was utilized in order to prevent seepage of water from the denitrification bed into surrounding soil while allowing gas products of the process to escape. The construction process of the excavated woodchip-bioreactor are shown in Figure 3.3.

Figure 3.3: The construction process of the denitrifying bioreactor evaluated in this study

3.2 Water Sampling and Analysis

Water samples were collected from the upstream and downstream flow control structures from December 7 through February 15. Data collection from the bioreactor was performed via Teledyne ISCO automated water samplers on a schedule ranged weekly to biweekly (predominantly weekly) which was dependent on the presence of water and/or flow in the control components. ISCO samplers (model 2900) were programmed to collect water on a daily basis by the plastic sample bottles with a capacity of 500ml. Samples were transferred to conical-bottom centrifuge tubes, and kept constantly frozen at -10°C prior to analysis.

Water quality analysis was conducted at the Biochemistry Laboratory, Oregon State University for determination of nitrogen species (NO_3^-, NO_2^- and NH_4^+) concentrations using a Shimadzu UV-Visible Spectrophotometer (model UV-1700). NO_3^- concentrations were analyzed with the VCl_3 / Griess method which is based on the procedure for biological samples described by Miranda et al. (2001). The principle of this assay is the reduction of NO_3^- to NO_2^- in an acidic VCl_3 solution combined with measurement of NO_2^- with Griess reaction in a single step. The estimation of NO_2^- levels formed during a timed incubation period is performed to determine enzymatic activity at a fixed temperature. This assay protocol is sensitive to detect NO_3^- concentrations of as low as 0.5 μM and involves the reaction of sulfanilamide and N-ethylenediamine dihydrochloride (Griess reagents) with sample media to measure the resulting absorbance photometrically at 540 nm.

NO_2^- concentrations present in the samples were determined through a method similar to the one applied for NO_3^- determination with the major exception of the addition of VCl_3 solution. Based on the procedure described by Hageman & Hucklesby (1971), the reaction of NO_2^- with sulfanilic acid and the aromatic amine 1-naphthylamine is expected to cause the formation of a deep red-colored azo dye under acidic conditions. After incubation at room temperature for 20 min, NO_2^- levels were measured photometrically at 540 nm.

Determination of NH_4^+ levels in the water samples was employed by a sensitive spectrophotometric procedure developed by Qiu et al. (1987). In the presence of sodium hypochlorite and sodium nitroprusside that serves as a catalyst, water-soluble NH_4^+ ion reacts with salicylate to form a blue-green colored dye that absorbs light at 697nm after an incubation period of 60 min at room temperature.

At the end of each water analysis detailed above, the resulting absorbance values were converted to concentration of nitrogen species as mg/L with the help of calibration curves created.

3.3 Simulating Drainage Discharge

In the estimation of theoretical HRT and load NO_3^- removal rate, volumetric flow rate through the bioreactor is one of the most significant parameters in addition to active flow volume and porosity of the carbon media. To date, flow rates observed in the denitrification bioreactor studies have been predominantly calculated through direct field monitoring. These measurements were conducted either by capturing the flow rates of water with the application of area velocity meters in the outlet tile drains connecting to inlet control structure or monitoring the water height levels using pressure transducers in both control structures in order to obtain hydraulic gradient along the length of the denitrification bed.

In this study, incoming tile drainage flow criteria were predicted by the latest version of Drainmod, a comprehensive process-based computer simulation model. Drainmod software employs a one dimensional soil-water balance in order to simulate agricultural drainage, surface runoff, evapotranspiration, infiltration, day-by-day basis water table depth and deep or lateral seepage from drainage area. In the soil profile, the evaluation of multicomponent drainage systems is performed based on the following subsurface and surface water balances respectively for any section of soil present in the midpoint between adjacent drains.

$$\Delta V_a = F - ET - DLS - DS \tag{3.1}$$

where, ΔV_a is the change in the water-free pore space or air volume for soil layer of

interest (cm), F is infiltration (cm), ET is the loss of water by evapotranspiration (cm), DLS is loss resulted from deep and lateral seepage (cm) and DS is the lateral drainage from (or sub-irrigation) the soil section.

$$P = F + \Delta S + RO \tag{3.2}$$

where, P is the precipitation (cm), F is infiltration entering the soil section of interest (cm), ΔS is the change in the volume of water stored on the surface (cm) and RO is the surface run-off during certain time increment. The water balances for unsaturated soil zone (vadose zone) are computed by Drainmod in order to estimate water table elevation and soil-moisture content at a point of interest located within the midway of two parallel drainage lines as illustrated in Figure 3.4.

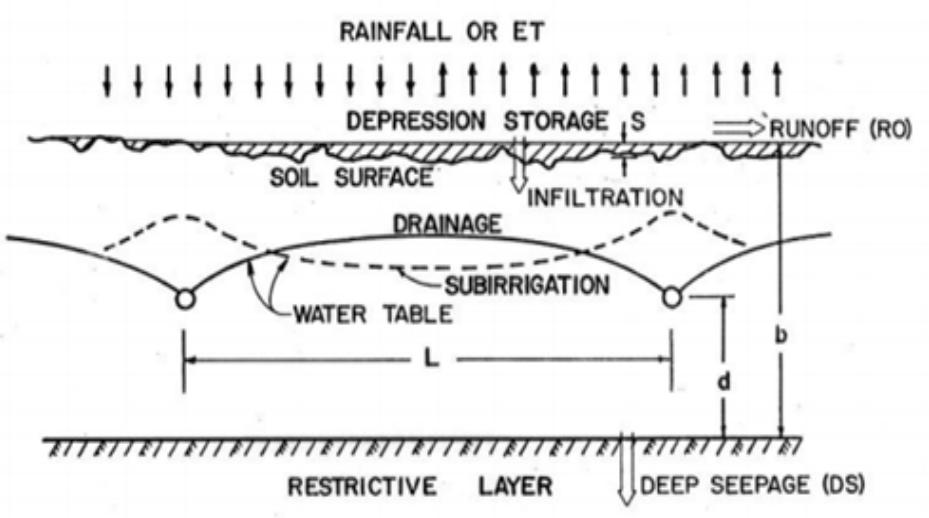

Figure 3.4: Principal hydrologic components considered by Drainmod in determination of drainage discharge (Skaggs et al., 2012)

For a user selected time interval, Drainmod simulation solves the equations 3.1 and 3.2 with the units of all hydrologic parameters specified in terms of depth (cm). Based on the surface and subsurface water balances stated above and provided input files that will be detailed later in this section, Drainmod model is capable to create outputs include subsurface drainage rates on daily, monthly and yearly bases.

The drainage flux through tiles is computed via Hooghoudt's steady state equation (Eq. 3.3) for the cases when the water table is below the surface level. The specific discharge rate in cm per hour is calculated in terms of the approximated hydraulic head in the drains and the elevation of water table at the midpoint of adjacent drains.

$$q = \frac{8Kd_e + 4Km^2}{L^2} \tag{3.3}$$

In equation 3.3 q represents the hourly drainage flux (cm/h), m is the midpoint water table height above the drain (cm), d_e is the equivalent depth between drains and the impermeable layer (cm), K is the effective lateral hydraulic conductivity (cm/h) and L is the distance between drains. Under fully-saturated conditions, on the other hand, Drainmod simulation uses the equation derived by Kirkham (1957) to predict subsurface drainage rate when the surface is expected to be ponded.

$$q = \frac{4\pi K(t + b - r)}{GL} \tag{3.4}$$

where, t is the depth of water ponded on the surface (cm), b is the actual depth from

surface to the tile drain (cm), r is the radius of the tile drain (cm) and G is a dimensionless parameter dependent on tile drain spacing and the depth from surface.

The predictive capacity of Drainmod hydrology tool is subject to a large extent on the reliability of input files that can be mainly categorized into three groups: meteorological data, soil hydraulic parameters and drainage system information. Input parameters related to mineral fertilizer applications and the detailed crop information would be required to simulate concentrations and transportation of nitrogen species present in tile drainage system. The Drainmod model was applied to a period of ten years (2008 to 2018) that includes data collection period for validation purposes mentioned before. The procedures followed in this study to create hydrological input parameters are summarized in the following sub-sections.

Soil Inputs

Site-specific soil water characteristics versus pressure head, drainage volume-water table depth relationship, the lateral hydraulic conductivity of each soil type present in the site above impermeable layer and parameters governing infiltration processes are primary soil inputs required to simulate hydrologic processes. These soil hydraulic input parameters can be measured through field measurements, but it is time-consuming, uneconomical and impractical for larger scale applications in particular. Therefore, bulk density values and soil physical properties include soil moisture content at -33 and -1500 kPa for the study area were obtained from Web Soil Survey provided by the USDA Natural Resources Conversation Service (Table 3.1). However, these properties are still need be processed in order to be utilized by a built-in soil utility program in Drainmod 6.1

that is executed to create required properly formatted soil input files. This embedded soil utility software is capable to estimate Green-Ampt infiltration parameters and the volume drained and upward-flux relationships, all as functions of water table depth using the van Genuchten-Mualem parameters estimated by a pedotransfer function and neural network software package, Rosetta (Schaap et al., 2001). Despite, its possible restrictions, Rosetta is one of the most widely used models to derive the van Genuchten-Mualem water retention properties, saturated hydraulic conductivity as well as unsaturated conductivity in accordance with a pore-size model created by Mualem (1976). Soil texture, water content and bulk density values obtained from online soil survey for the drainage area were passed to the Rosetta software to create essential outputs for proceeding Drainmod simulation. The predicted output parameters of Rosetta include the saturated water content (θ_s), the residual water content (θ_r), the saturated hydraulic conductivity (k_{sat}), a fitted matching point at saturation (K_0), empirical curve shape factors and pore tortuosity/connectivity parameters are presented in Table 3.2.

Table 3.1: Soil physical parameters obtained from Web Soil Survey for the study area

Bottom Depth of Layer (cm)	Sand %	Silt %	Clay %	Bulk Density at 1/3 Bar (g/cm3)	θ_{33} (cm3/cm3)	θ_{1500} (cm3/cm3)
12	7	65	28	1.27	0.323	0.203
38	6	60	34	1.29	0.344	0.208
66	5	53	42	1.31	0.359	0.235
89	7	50	43	1.31	0.367	0.238
125	8	52	40	1.3	0.345	0.215

Table 3.2: Predicted soil hydraulic properties by Rosetta model

Bottom Depth of Layer (cm)	θ_s (cm3/cm3)	θ_r (cm3/cm3)	α (1/cm)	n (-)	K_{sat} (cm/day)	K_o (cm/day)	L (-)
12	0.473	0.086	1.220	1.285	32.92	7.32	-1.57
38	0.479	0.084	1.215	1.299	20.75	4.30	-1.01
66	0.488	0.094	1.241	1.252	14.30	5.05	-1.72
89	0.490	0.092	1.235	1.254	14.19	4.44	-1.54
125	0.482	0.087	1.223	1.281	16.01	4.70	-1.26

Based on the predicted soil properties through Rosetta and the site-specific data acquired from online soil survey, three types of soil input files were generated to run Drainmod simulation. The first soil file (extension .SIN) is mandatory for all Drainmod projects regardless of the purpose of the study. This file consists of major soil hydrology data which includes air or water free pore volumes corresponding to various water table elevations, soil water characteristic curve, capillary movement versus water table depth, and Green-Ampt infiltration parameters. The soil file distinguished by the extension of .MIS primarily utilized in the salinity and nitrogen simulations, and it gives more detailed soil data with changing soil temperature. The last soil input file (.WDV) stores drainable water volumes against corresponding water table depths.

Weather Inputs

The required climatological data to predict subsurface drainage volume by Drainmod consist of daily maximum and minimum air temperature, hourly precipitation,

and daily potential evapotranspiration (PET) records through simulation period. The daily precipitation and temperature observations with a spatial resolution of 4km were obtained from the PRISM Climate Group (http://www.prism.oregonstate.edu/). To create correctly formatted temperature (.TEM) and precipitation (.PET) input files, an embedded weather utility software in Drainmod was used. The software is capable to convert columnar climatic data to essential Drainmod input format. In order to estimate hourly rainfall in millimeter from the observed precipitation sums on a daily basis, the utility was programmed to distribute equal amount of rainfall (uniform distribution) over 8 hours (from 14 to 22 h). The required daily potential evapotranspiration values can be incorporated into the simulation through either a .PET file or default feature of Drainmod that use the Thornthwaite method. The PET values for this project were estimated using the Thornthwaite method that requires firstly calculate the heat index (I) (Eq. 3.5). This parameter was then entered in the simulation along with the latitude of the study area to specify monthly PET factors.

$$I = \sum_{i=1}^{12} \left(\frac{T_i}{5}\right)^{1.514} \tag{3.5}$$

where, T_i is the monthly heat indices in degrees Celsius. The estimated annual heat index (I) is replaced in the following equation.

$$PET = 16\left(\frac{L}{12}\right)\left(\frac{N}{30}\right)\left(\frac{10T_a}{I}\right)^{\alpha} \tag{3.6}$$

where,

$$\alpha = (6.75E^{-7})I^3 - (7.71E^{-5})I^2 + (1.79E^{-2})I + 0.49239$$

PET value in Drainmod routine is estimated based on the equation 3.6 where, T_a stands for the mean daily temperature (°C), L is the average length of the day (hours), N is the number of days of the month being calculated and α is the empirical fitting parameter.

Drainage System Parameters

Drainmod requires users to describe the design of the subsurface drainage system in addition to more specific factors that can influence discharge intensity such as drainage coefficient, maximum surface storage and Kirhkam's depth under the project design settings. The maximum drainage rate that can be observed in a day is set by the drainage coefficient which is typically dependent on the drainage layout, the effective radius of the drain, and the type of perforations. Maximum surface storage (S_m) stands for the maximum depth of ponded water on the surface that may runoff with additional excess. Lastly, Kirkham's depth for flow to drains represents the depth of surface storage when the soil profile is fully saturated and lateral movement of ponded water may not occur. The selected values for the Drainmod simulation based on site-specific parameters and field observations are presented in Figure 3.5.

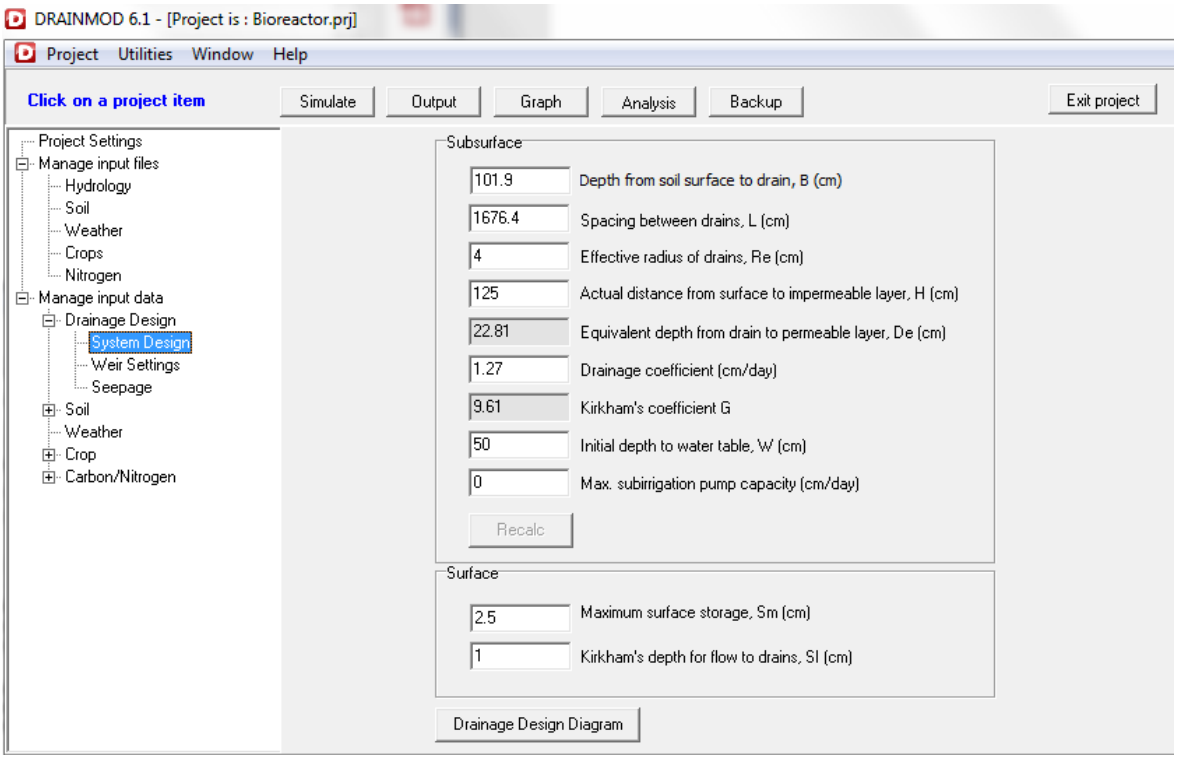

Figure 3.5: Screenshot of the project window presenting drainage design data used in the Drainmod Hydrology Simulation

3.4 Predicting Temperature Effect on Nitrate Removal Rates

It is well known that denitrification as an enzyme catalyzed reaction in a bioreactor is subject to the alterations in drainage water temperature. In order to incorporate temperature dependency of the process into nitrate removal model, onset Hobo temperature monitoring sensors were deployed at the bioreactor inlet and outlet control structures to record water temperatures at 30 min intervals. Average air temperatures were also measured via another sensor installed over the surface of the bioreactor. The graphic representation of recorded temperatures from each sensor throughout the sample collection period were shown in Figure 3.6.

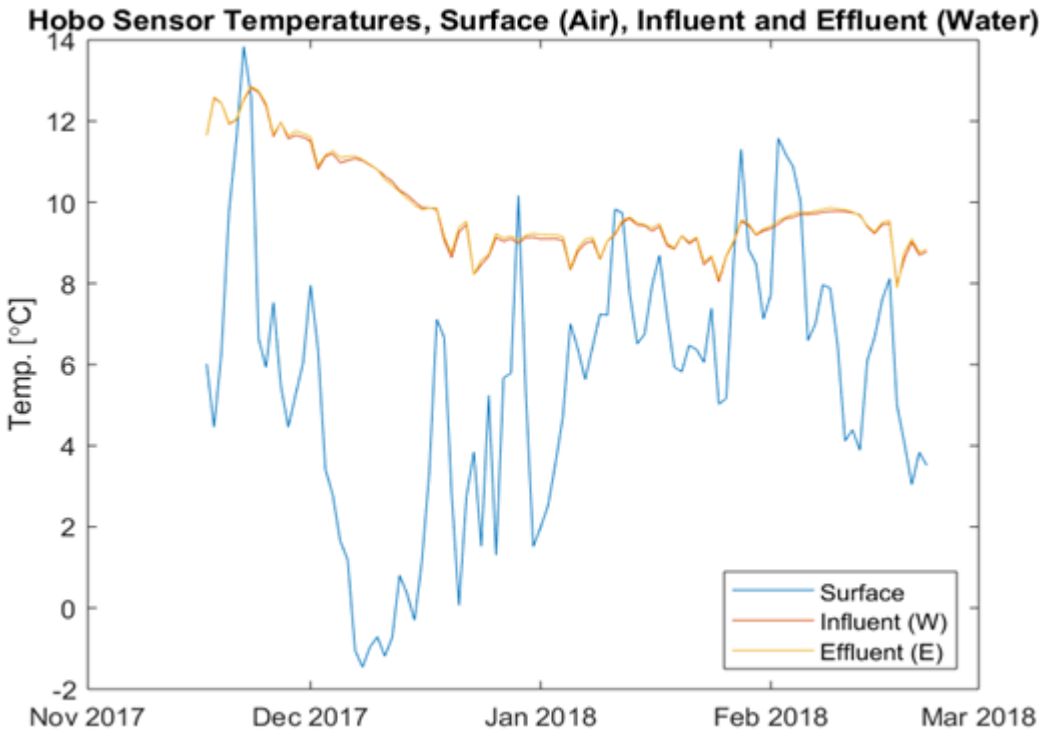

Figure 3.6: Recorded influent, effluent and air temperatures through sampling period

To date, the temperature sensitivity of nitrate removal process that can be observed in bioreactors have been described by the Arrhenius equation. This model suggests an exponential rise in the rate of denitrification thanks to increased kinetic energy possessed by substrates of the reaction at relatively higher temperatures. Arrhenius-type functions provide an accurate thermodynamic representation of measured denitrification rates, but there are still discrepancies in the ability of these theories in terms of fitting observed data. The classical Arrhenius behavior is known to be valid up to an optimum temperature (T_{opt}) beyond which enzyme denaturation and/or aggregation occurs.

Hobbs et al, (2013) presented macromolecular rate theory (MMRT), which answers questions arising from the Arrhenius equation by incorporating heat capacity (C_p) into the rate function; corresponding to the enzyme stability and curvature above temperature optima. They hypothesized that a large and negative change in C_p value unexpectedly has a profound influence on catalytic temperature dependence of all microbial processes in the absence of protein denaturation. The MMRT function accounts for a rate decline above T_{opt} that attributed to decreased enzyme activity unlike Arrhenius-type functions. The natural log form of MMRT equation:

$$lnk = ln\left(\frac{k_B T}{h}\right) - \frac{\left[\Delta H^{\ddagger} + \Delta C_P{}^{\ddagger}(T - T_0)\right]}{RT} + \frac{\left[\Delta S^{\ddagger} + \Delta C_P{}^{\ddagger}(lnT - lnT_0)\right]}{R} \quad (3.7)$$

where, k_B is the Boltzmann's constant, h is the Planck's constant, $\Delta C_p{}^{\ddagger}$ is the difference in heat capacity between the reactants and the transition state at constant

temperature, in turn $\Delta S^{\ddagger}$ is the change in entropy and ‡ stands for the transition state. For the reactions where $\Delta C_p^{\ddagger}$ is large and negative, the temperature response will differentiate considerably from what would be calculated by the Arrhenius function. On the other hand, the temperature response is known to be predicted accurately based on Arrhenius equation when $\Delta C_p^{\ddagger}$ is close to zero since the free energy of the system will be independent of temperature. MMRT was recently applied successfully by Schipper et al, (2014) to a variety of soil microbial processes include denitrification using experimental data reported in the literature. Total Denitrification N flux was reported as the emission rate of nitrous oxide that comprises both N_2O–N and N_2–N since the experiment was set up to inhibit the microbial reduction of N_2O to N_2 (Figure 3.7).

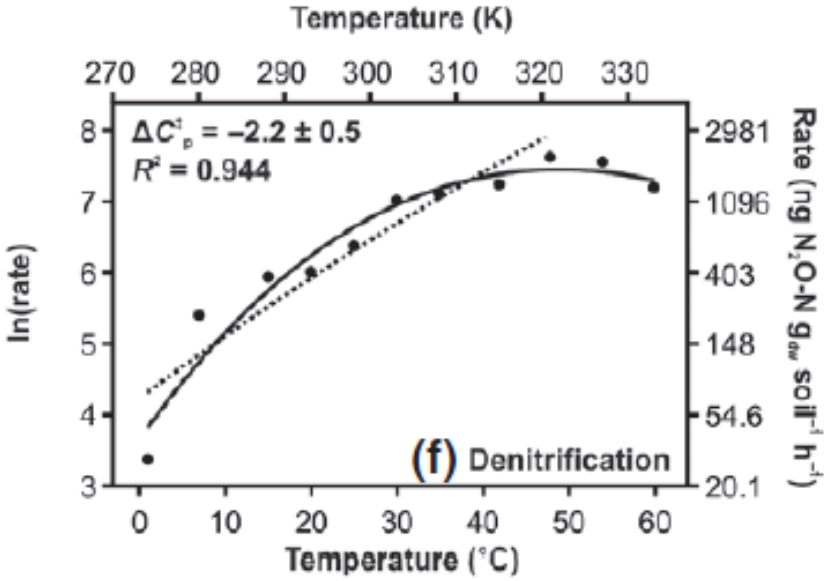

Figure 3.7: The fit of the MMRT function to denitrification process (Schipper et al., 2014)

The denitrification rate as a function of temperature were presented by the solid line in the Figure 3.7 which depict that the reaction rate will start declining after the temperature optima at around 47°C. The standard Arhenious equation (the dashed line) was also fitted to empirical data up to T_{opt}. In the NO_3^- removal model equation that will be discussed further in the data analysis section, approximated denitrification rates based on MMRT function were obtained by extracting data points from the solid line in the Figure 3.7 via DataThief III (www.datathief.org).

3.5 Data Analysis

The percent removal of NO_3^- was calculated as the difference between observed influent and effluent NO_3^- concentrations ($[NO_3]_{in}$ and $[NO_3]_{out}$) divided by nitrate load of inlet water (mg/L) (Eq. 3.8).

$$\text{Measured } NO_3\text{-N mass reduction (\%)} = \frac{[NO_3]_{in} - [NO_3]_{out}}{[NO_3]_{in}} 100\% \quad (3.8)$$

Assuming that drainage flow entering the bioreactor is darcian, then volumetric flow rate (Q) was determined by multiplying q (specific discharge or darcian velocity) (m/day) that is predicted by Drainmod hydrology simulation by drainage area of the 7.6 ha field. In accordance with the influent volumetric flow rates (m^3/day), actual daily NO_3^- load reductions (g N/ m^3/d) were calculated using the following equation.

$$\text{Measured } NO_3\text{-N removal rate} = \frac{Q([NO_3]_{in} - [NO_3]_{out})}{V} \quad (3.9)$$

where, V is the active flow volume of the woodchip bioreactor (20.84 m^3).

Furthermore, the effluent NO_3^- concentration in mg/L was simulated based on the Equation 3.10 that incorporates water quality analysis and simulated drainage discharge into the denitrification rates as a function of temperature based on MMRT function.

$$[NO_3]_{out} = -r_{NO_3}(T)\,\frac{Vn_e}{Q} + [NO_3]_{in} \quad (3.10)$$

In the model equation (Eq. 3.10), $r_{NO_3}(T)$ is the reported temperature dependent denitrification rates (k) in mg N $L^{-1}h^{-1}$ extracted from Figure 3.7 (with units converted for consistency), n_e is the effective (drainable) porosity that was assumed to be 0.7 as recommended in the USDA national conversation practice standard for denitrification bioreactor design. For the subsequent sections of this thesis, the term 'first model' refers simulations conducted based on the equation 3.10 to predict effluent NO_3^- concentrations in mg/L.

3.6 Reactive Transport Modeling of the Bioreactor by MIN3P

Microbially mediated NO_3^- reduction in variable saturated flow through the bioreactor was simulated by a multicomponent reactive transport code, named MIN3P. The model was specifically developed to address mass balance equations for adjective-diffusive

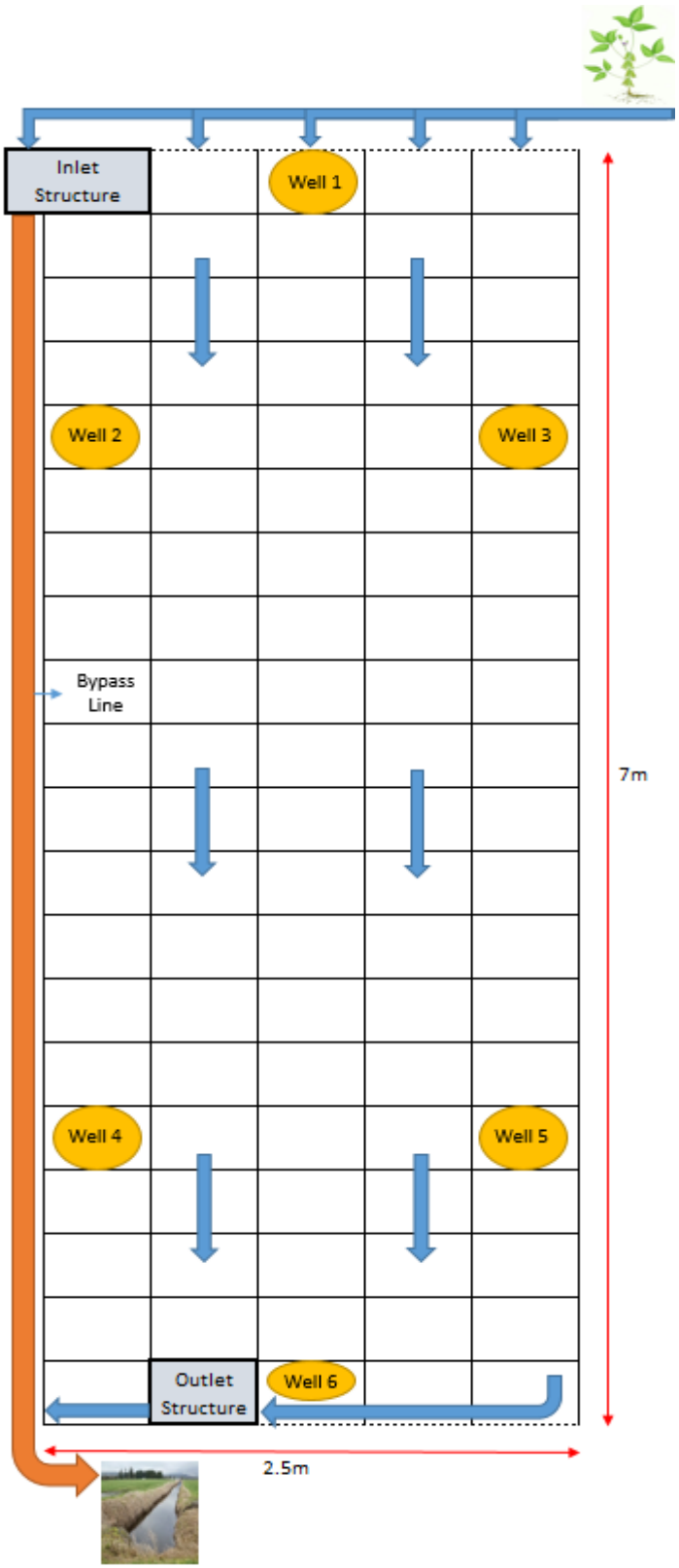

Figure 3.8: Schematic of the bioreactor indicating 2D flow and spatial discretization

solute and gas transfer based on Richard's equation for partially-saturated media, thus it is well-suited for the application of denitrification bioreactors. The block-centered finite volume code, furthermore, employs the global implicit solution assuming that physical transport and biochemical reactions among surface, solid, gaseous and dissolved species occur simultaneously.

Spatial discretization across the domain can be specified in one, two, and three dimensions in line with the finite difference method. In this study, the denitrification reactor is partitioned into 20 equally spaced control volume in the x direction and 5 of that in the y direction for a 2D-simulation (Figure 3.8).

As presented in the figure 3.8, the finite volume grid is discretized to consist of 100 cells starting from the one that stands for the influent control structure. Concentrations that are estimated at x = 0 and 7 m, corresponding to the influent and effluent boundaries, respectively. Numbering of the control volumes is performed for the simulation along the length of the bioreactor first (x-direction), then through the width (y-direction). The diagram also provides the placement of six monitoring wells installed during construction in the woodchip trench. Each well is represented by a control volume in order to predict NO_3^- concentrations that could be observed at these positions.

The initial condition for the variable saturated flow along the whole domain is specified by a hydraulic head value of 0.2 m that is approximately equal to the diameter of the perforated pipes. The porosity along the entire homogeneous domain is set to a constant value of 0.7 as utilized in the first model. The inflow that covers the entire width of the bioreactor is assigned as the Neumann transient boundary condition by providing an external file includes daily drainage discharges in meter per second predicted by

Drainmod, while the 'outflow boundary' is set as constant hydraulic head of 0.0 m (Dirichlet condition). The top and bottom layers of the bioreactor are assumed to be no-flow boundary, thus impermeable. The hydraulic conductivity of the porous media is specified as a uniform value of 9.5 cm/s for each spatial direction. The measured daily concentrations of nitrogen species (Nitrate, nitrite, and ammonium) at inlet control structure were used to define the chemical composition of initial and inflow boundary waters of the domain. The biochemical system is composed of 9 primary components, 3 secondary species, 2 gases and biomass components (Table 3.3). Concentrations for CO_3^{2-}, N_2 (aq), biomass components ($C_5H_7O_2N$ for active and $C_5H_7O_2N$ (d) for dead biomass), and CH_2O as electron donor are those reported in the study of Molins et al. (2015), while the value of DO concentration present in drainage discharge is the most commonly detected value based on the relevant literature. Initially, denitrifying bacterial populations were assumed to uniformly distribute in the solid-state carbon media.

Table 3.3: Initial and boundary conditions of the domain for reactive transport

Parameter	Inflow Boundary	Initial Condition	Unit
H^+	7.0	7.0	pH
O_2 (aq)	2.50E-04	2.50E-04	[mol/L]
CO_3^{2-}	1.25E-03	1.25E-03	[mol/L]
CH_2O	1.50E-33	1.50E-03	[mol/L]
NO_3^-	1.25E-03	1.30E-04	[mol/L]
NO_2^-	1.00E-33	1.00E-33	[mol/L]
N_2 (aq)	1.00E-33	1.00E-33	[mol/L]
NH_4^+	4.44E-05	4.44E-05	[mol/L]
$C_5H_7O_2N$	1.00E-15	5.00E-05	[mol/L]
$C_5H_7O_2N$(d)	1.00E-15	1.00E-15	[mol/L]

In the Table 3.3, concentrations of N species are averages of measured data through monitoring period, and these values were used just for the spatial profile simulations of the bioreactor. However; nitrate, nitrite and ammonium concentrations were updated on a daily basis to predict effluent NO_3^- concentrations (control volume 40), then compare the results with those simulated by the first model. The rest of the values stated on the table were utilized for all MIN3P simulations. The code was executed with a minimum time step of 0.01 hour (corresponding to 2400 time steps for 24-hour simulations) to prevent from convergence failures.

CHAPTER 4. RESULTS AND DISCUSSION

4.1 Predicted Drainage Discharge and Hydraulic Retention Times

Theoretical HRT in a denitrification bioreactor is greatly subject to alterations in drainage discharge rates. As described in the methodology section, specific discharge rates in cm/day were simulated by Drainmod model. Drainage discharge entering the bioreactor was plotted to compare with the precipitation amounts during the observation period (Figure 4.1). Predicted drainage flow rates elevated substantially in response to recorded rainfall values during the three month study. Monthly precipitation amounts from December 2017 through February 2018 were 87, 170 and 69.5 mm, while monthly sums for tile drains were simulated to be 77, 128 and 38 mm. Taking into consideration the monthly rainfall and drainage discharge amounts as well as Figure 4.1, it may be suggested that simulated discharge followed the overall trend of precipitation events to some extent.

HRTs of the bioreactor and active flow volume are known to be highly dependent on the volumetric flow rates entering the bioreactor apart from the effective porosity that was assumed to remain constant at 0.7 through monitoring period (Eq. 4.1)

$$\mathrm{HRT} = \frac{\mathrm{V}n_e}{\mathrm{Q}} \tag{4.1}$$

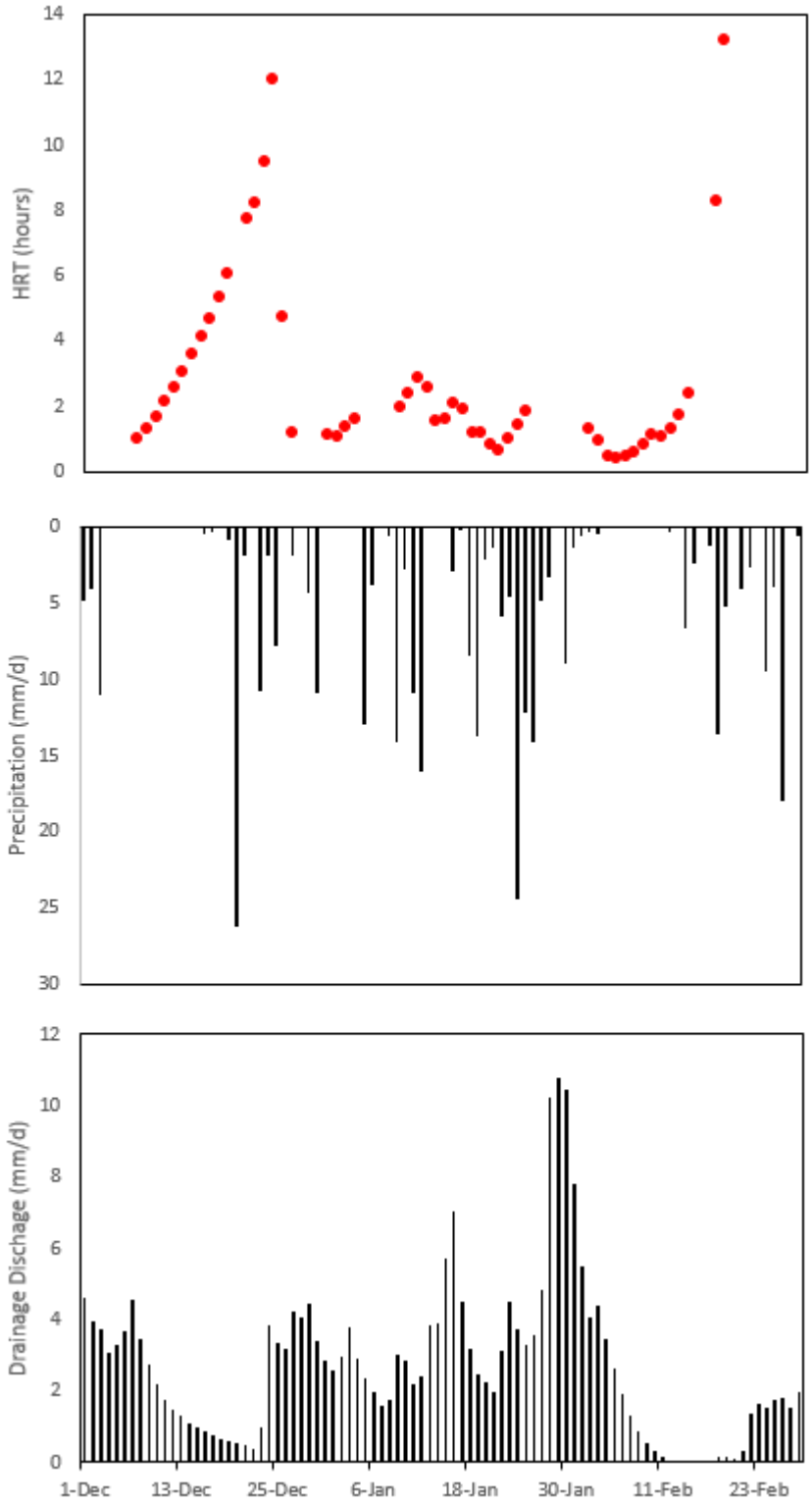

Figure 4.1: HRTs, daily precipitation records, and simulated tile flow into bioreactor through the study period

The theoretical HRTs estimated based on the simulated specific discharge rates ranged from approximately 1 h to 13 h (3.2 h average). These findings also suggest that retention times in the bioreactor may not have been long enough to provide complete nitrate reduction during high flow periods considering the recommended retention time of at least 3 hours at the peak flow capacity (USDA-NRCS, 2015). As illustrated in Figure 4.1, HRTs are inversely proportional to predicted drainage discharge rates.

4.2 Nitrate Mass and Percentage Removals

Tile flow data gained via Drainmod simulation were combined with observed influent and effluent concentrations in order to estimate NO_3^- load reductions through sampling period. NO_3^- concentrations in the agricultural tile flow varied in the range from 2 to 13 mg/L (8 ppm average) while measured NO_3^- in the downstream control structure were between 1 and 12 mg/L (on average 6 ppm) during the non-growing season (December to February) as shown in Figure 4.2a. NO_3^- removal rates were expressed using the equation 3.9 that accounts for the grams of NO_3^- removed in a day taking into account the total volume of the bioreactor (21 m^3). The average load reduction achieved in the study was 21 g N/ m^3/d, and ranged from 1 to169 g N/ m^3/d, that was beyond most of the published values in the literature. Bell et al. (2015), for instance, reported an average NO_3^- load reduction rate of 11.6 g N/ m^3/d. On the other hand, the findings of this study are quite lower than the monthly NO_3^- removal values of 23 to 44 g N/ m^3/d in the first year of operation reported by David et al. (2016). When NO_3^- mass removals were plotted as a function of increasing retention times, no significant correlation was found between HRT

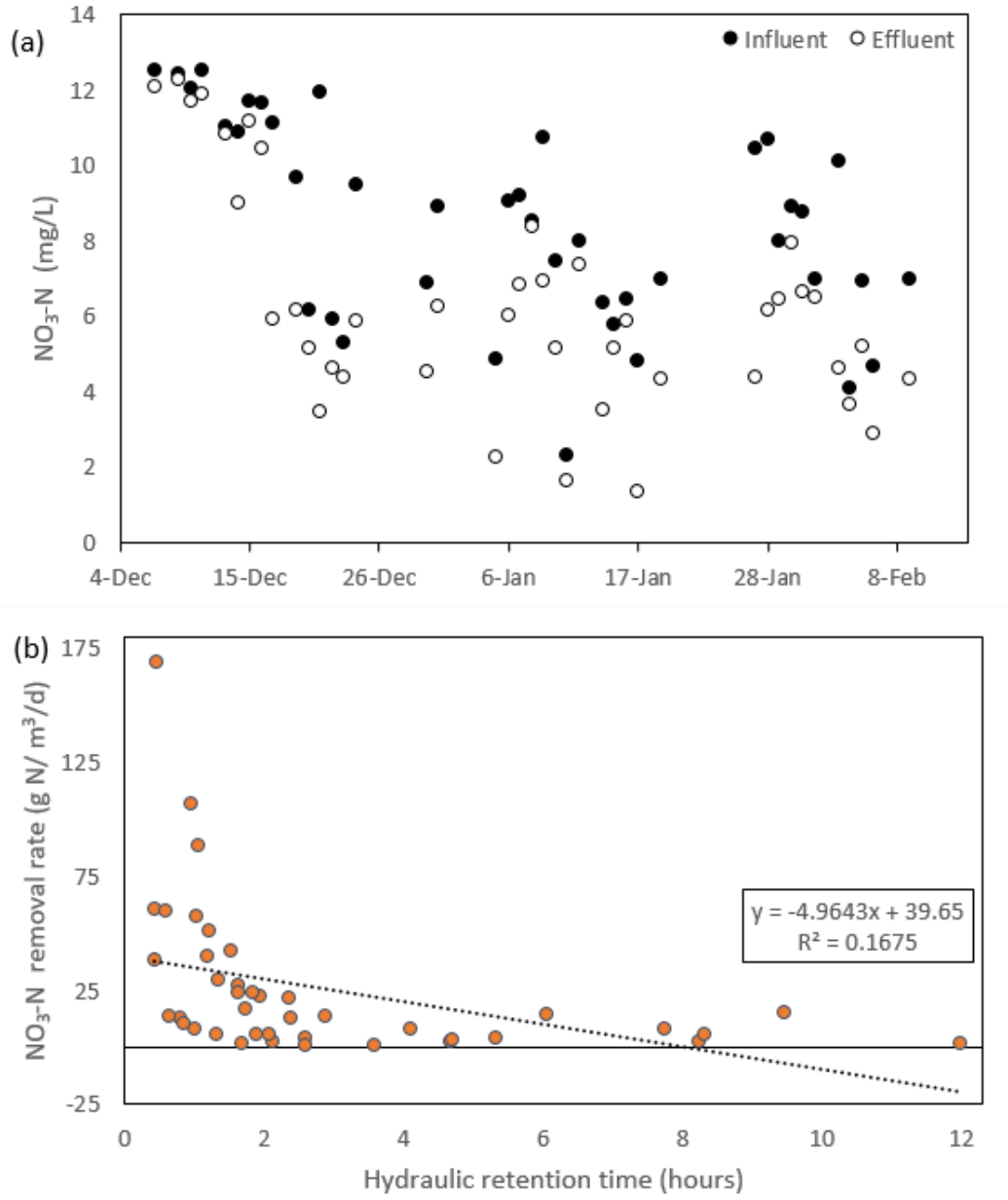

Figure 4.2: Influent and effluent NO_3^- concentrations (a), and NO_3^- mass removal rates as a function of HRTs (b)

and NO_3^- load reduction (Figure 4.2b).

In addition to volumetric NO_3^- removal rates, the performance of the bioreactor was evaluated on the basis of NO_3^- percentage removals as well. Considering the aforementioned mean influent and effluent NO_3^- concentrations observed through the study period (8 and 6 ppm, respectively), the calculated average NO_3^- percent mass reduction was 26% (Figure 4.3b). The NO_3^- percent attenuation efficiency varied significantly throughout the observation period with minimum and maximum percent removals of 1% and 72% in turn. These results fell within the range of percent reduction values reported in field-scale denitrification bioreactor studies. Christianson et al. (2012) evaluated the performance of four field-scale horizontal flow bioreactors based on two years of water quality data, and they concluded that percent reduction of the influent NO_3^- ranged from 12 to 76% (mean 45%). Based on the findings of that study, the alterations in NO_3^- percent removal were attributed to drainage water temperature and retention times. Woli et al. (2010) found an average percent removal of 33% for two woodchip filled bioreactors located in east-central Illinois.

The effect of drainage water temperature on percentage NO_3^- reduction was also evaluated throughout the study period. Relatively large or insufficient percent removal rates were observed regardless of water temperatures. It was anticipated that percent NO_3^- reductions are likely to be greater with increasing water temperatures since higher temperatures are known to precipitate higher growth rates of denitrifying microorganisms in the soil environment. However, increasing water temperatures did not strongly correlated with increased percent removal as presented in Figure 4.3a since the NO_3^-

attenuation performance of the bioreactor was evaluated under a low temperature range (averaging 10°C) during the study. Seasonal variation in the organic carbon availability thanks to changes in temperature and moisture content of the denitrification bed may be the major cause of this unexpected result (Porter et al., 2015). In a field-scale study, Hassanpour et al. (2017) investigated paired denitrifying bioreactors constructed in three different landscapes in New York State for a three-year period. They concluded that NO_3^- reduction rates did not vary significantly when water temperatures were below 16°C, although a dramatic increase was reported at temperatures above 16°C at all field trials.

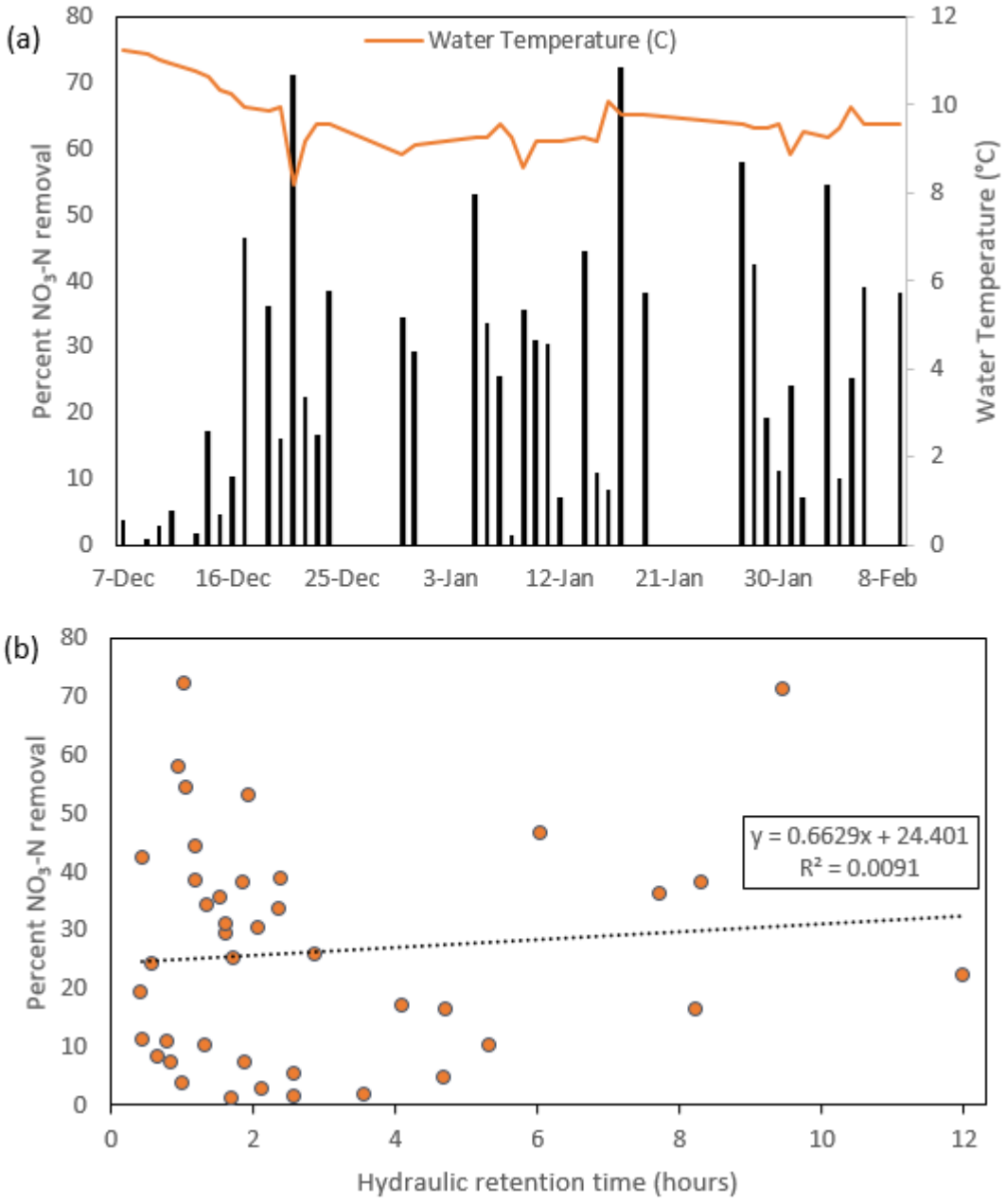

Figure 4.3: NO_3^- percent reduction and water temperature (a), and NO_3^- percent removal rates as a function of HRT (b)

4.3 Model Results

The effluent nitrate concentrations were predicted using Drainmod simulation outputs (drainage discharge rates) and temperature-dependent NO_3^- removal rates based on the equation 3.10. Reactive transport modeling in the bioreactor was performed by MIN3P code that provides the examination of the concentrations of nitrogen species along the spatial dimensions of the system. The bioreactor for the 2D simulation is defined to consist of 100 control volumes, with a uniform horizontal grid discretization of 0.35 m in length and 0.5 m in width to predict NO_3^- levels in monitoring wells, furthermore. In order to validate the applicability of both the first model and MIN3P code, simulated bioreactor effluent NO_3^- concentrations were benchmarked against the actual observed values through the study period. The validation procedure was undertaken to estimate the goodness-of-fit between measured and predicted results using the coefficient of determination (R^2) and the Nash-Sutcliffe efficiency (NSE) (Nash & Sutcliffe, 1970) as the model evaluation statistical metrics. The NSE coefficient was calculated in a form as presented in equation 4.2.

$$NSE = 1 - \frac{\sum(C_{obs} - C_{sim})^2}{\sum(C_{obs} - \overline{C_{obs}})^2} \tag{4.2}$$

where, C_{obs} is the observed effluent NO_3^-, C_{sim} is the simulated effluent NO_3^-, and $\overline{C_{obs}}$ observed mean effluent NO_3^- concentrations in mg/L. An NSE coefficient of 1 stands for a perfect fit of simulated results to the measured data, while NSE values lower than

zero (NSE < 0) indicate that the predictive power of the model is not even as high as the mean of the measured data. In this study, the model results were considered as satisfactory when the NSE coefficient was greater than 0.5 and/or $R^2 > 0.6$ (Santhi et al., 2007).

Figure 4.4 illustrates a comparison between simulated NO_3^- concentrations that were produced by the first model and measured data in the effluent of the bioreactor. Even though a few of the simulated results fluctuate on a random basis, the model captured the overall variation trend in the experimental data. The predicted NO_3^- percent removal efficiencies were within 20% of the results from monitored data and validated with a Nash-Sutcliffe coefficient value of 0.506 that was slightly above the predetermined threshold.

The MIN3P code evaluation resulted in a coefficient of determination value of 0.416 and NSE coefficient of 0.043 that did not indicate acceptable model performance comparatively based on the validation criteria mentioned before. Even though MIN3P model outputs were not as accurate as those simulated by the first model, these predictions also explained the general dispersion of observed data through monitoring period to a considerable extent (Figure 4.5). The average NO_3^- percent reduction based on MIN3P predictions was higher than observed removal efficiency (40.40 and 26, respectively). The MIN3P model presented in this study was executed using the kinetic parameters and rate constant that were estimated in a biostimulation column experiment for microbially mediated denitrification reaction (Molins et al., 2015). In that experiment, they used acetate as electron donor which is expected to permit rapid denitrification unlike less labile organic carbon forms like woodchips. This was interpreted as the major cause led to overestimated NO_3^- removal performance by MIN3P simulation. For comparison, the

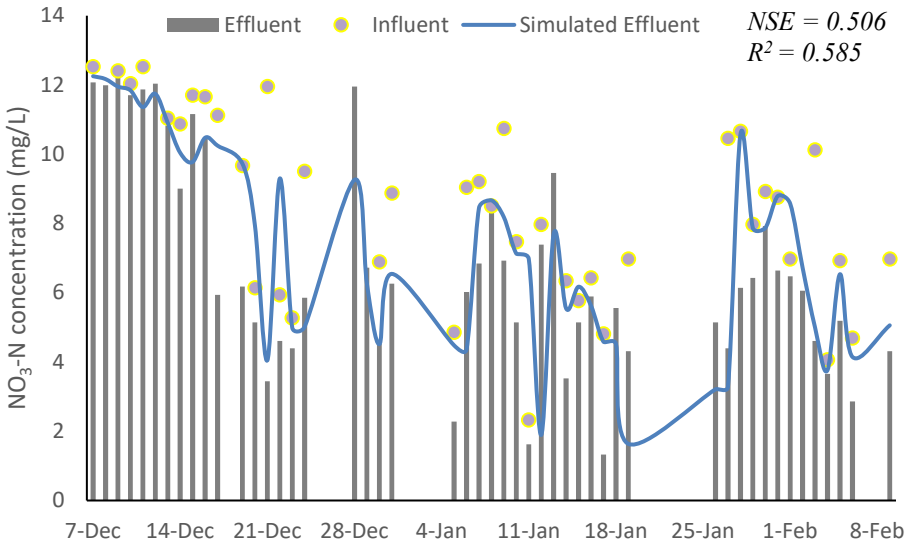

Figure 4.4: Observed influent and effluent NO_3^- concentrations in the bioreactor control structures and simulated effluent via first model

predicted effluent NO_3^- with 10-fold lower reaction rate was also fitted to data. As expected, it would contribute to better model performance. (NSE = 0.897, R^2 = 0.530).

The MIN3P code was run with a maximum time step of an hour in order to obtain breakthrough curves at the approximate locations of monitoring wells and concentration profile of NO_3^- along the length of the bioreactor with total a simulation interval of 24 h, as shown in Figures 4.6 and 4.7. The simulated NO_3^- concentrations almost remain constant through the width of the denitrification bed (data not shown), thus the model results for monitoring well 3 and 5 were not demonstrated in Figure 4.6 since they would have nearly the same breakthrough curves with well 2 and 4, in turn (see Figure 3.9). An immediate explanation is that the perforated pipe at inflow boundary distributes the incoming drainage water uniformly along the entire width of the bioreactor. The exhibited NO_3^- concentration profile in the x direction at hour 24 demonstrates that almost entire NO_3^- reduction takes place within approximately 2.6 m of the denitrification bed, then NO_3^- levels remain stable at 1.73 mg/L in the rest of the domain. Simulated breakthrough curves of simulated NO_3^- concentration at monitoring wells show excellent agreement with concentration profile (Figure 4.7). The monitoring wells (4 and 6) have exactly the same NO_3^- levels through the whole simulation period while at monitoring well 2 that is 1.75 m from the inflow boundary, NO_3^- concentrations are predicted to be around 1.77 mg/L at the end of the simulation period (24 h) what could be expected based on C profile. Because spatial analysis are in agreement in terms of NO_3^- dispersion along the length of the bioreactor, it is believed that inflow NO_3^- is predominantly removed within the first few meters of the bioreactor due to a large accumulation of biomass near the inlet.

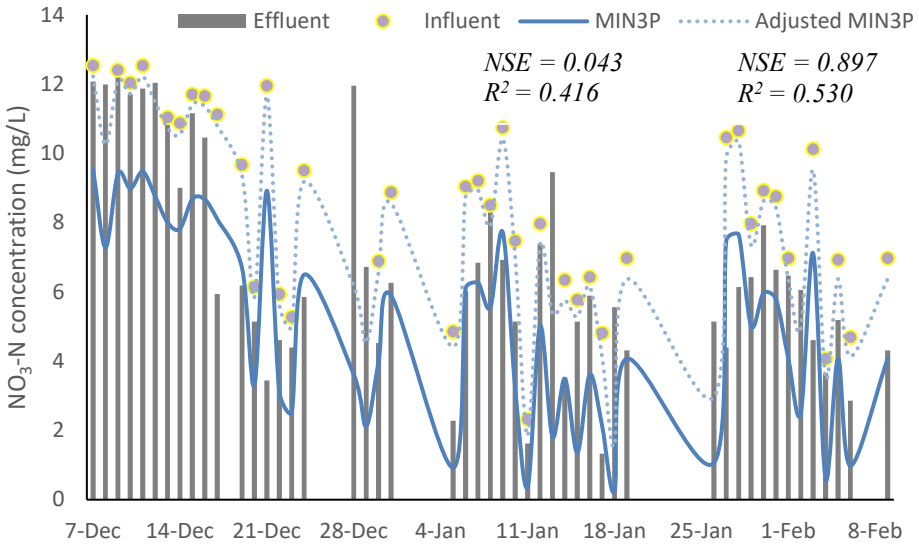

Figure 4.5: Observed influent and effluent NO_3^- concentrations in the bioreactor control structures and simulated effluent via MIN3P

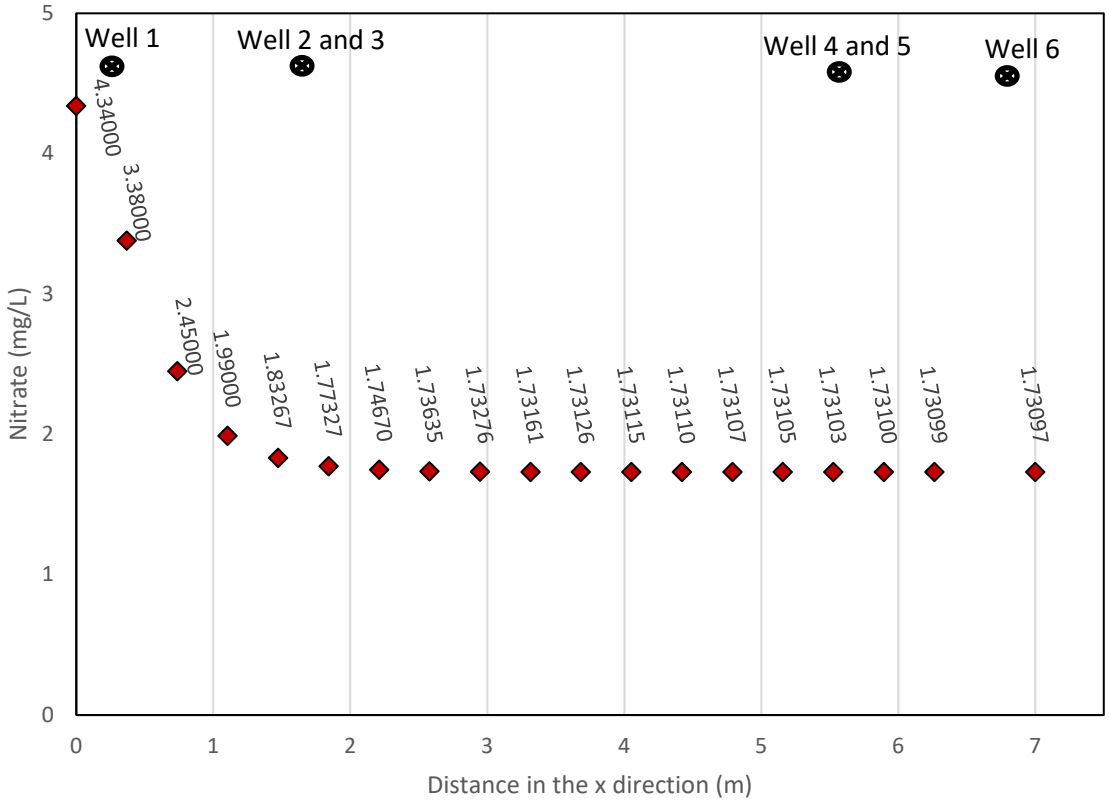

Figure 4.6: Simulated NO_3^- concentrations along the length of the bioreactor at 24 hours

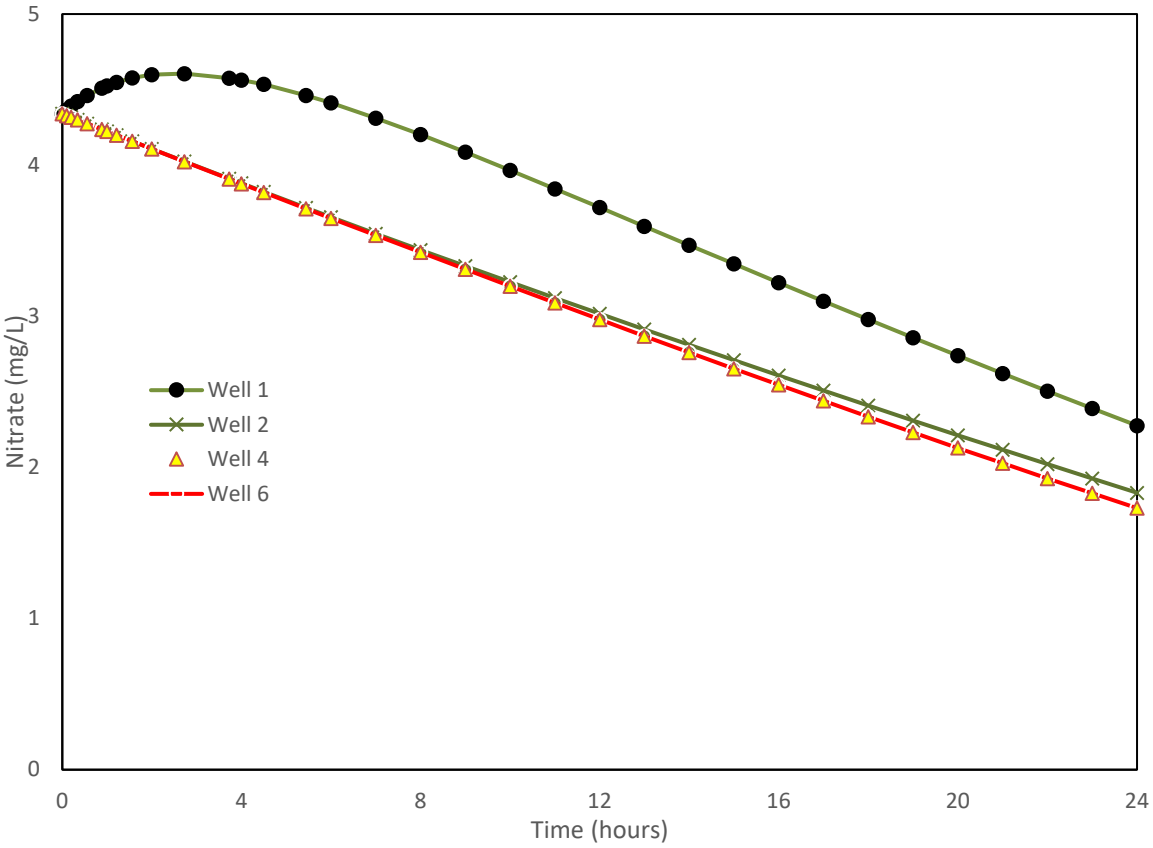

Figure 4.7: Simulated NO_3^- concentrations at monitoring wells as a function of time

4.4 Sensitivity Analysis

Sensitivity analysis requires to examine the relative magnitudes of changes in the model outputs with respect to fluctuations in the values of input variables. Denitrification process in the bioreactor is known to be dependent on a set of factors as detailed in the section of performance controlling parameters. The sensitivity analysis was performed on monitored or approximated inputs to identify the most influential parameters for the first model and MIN3P routine independently.

For the equation 3.10 (first model), Monte Carlo simulation was executed using selected stochastic variables include influent NO_3^- concentration, HRT and temperature. Monte Carlo methods are based on the parent distribution of each random variable that can be specified by providing standard deviation (STD) and mean as priori. The sensitivity of a model against selected input parameter or variable is dependent on the probability distribution of the uncertainty in the input as well as structure of the model. The monitored temperature data, inlet NO_3^- concentrations and simulated drainage effluent were utilized to characterize parent probability distributions (domains of possible inputs) to run repeated trials (in this case 10000 values for each parameter). Randomly generated outcomes based on the priori of parent domains were demonstrated for each equation variable (Figure 4.8). In univariate Monte Carlo simulations, individual parameters were allowed to vary on a random basis while all other inputs were held constant at measured or predicted averages to estimate whether the impact of the parameter of interest on effluent NO_3^- concentrations is statistically significant. In addition to determining the independent effect of each

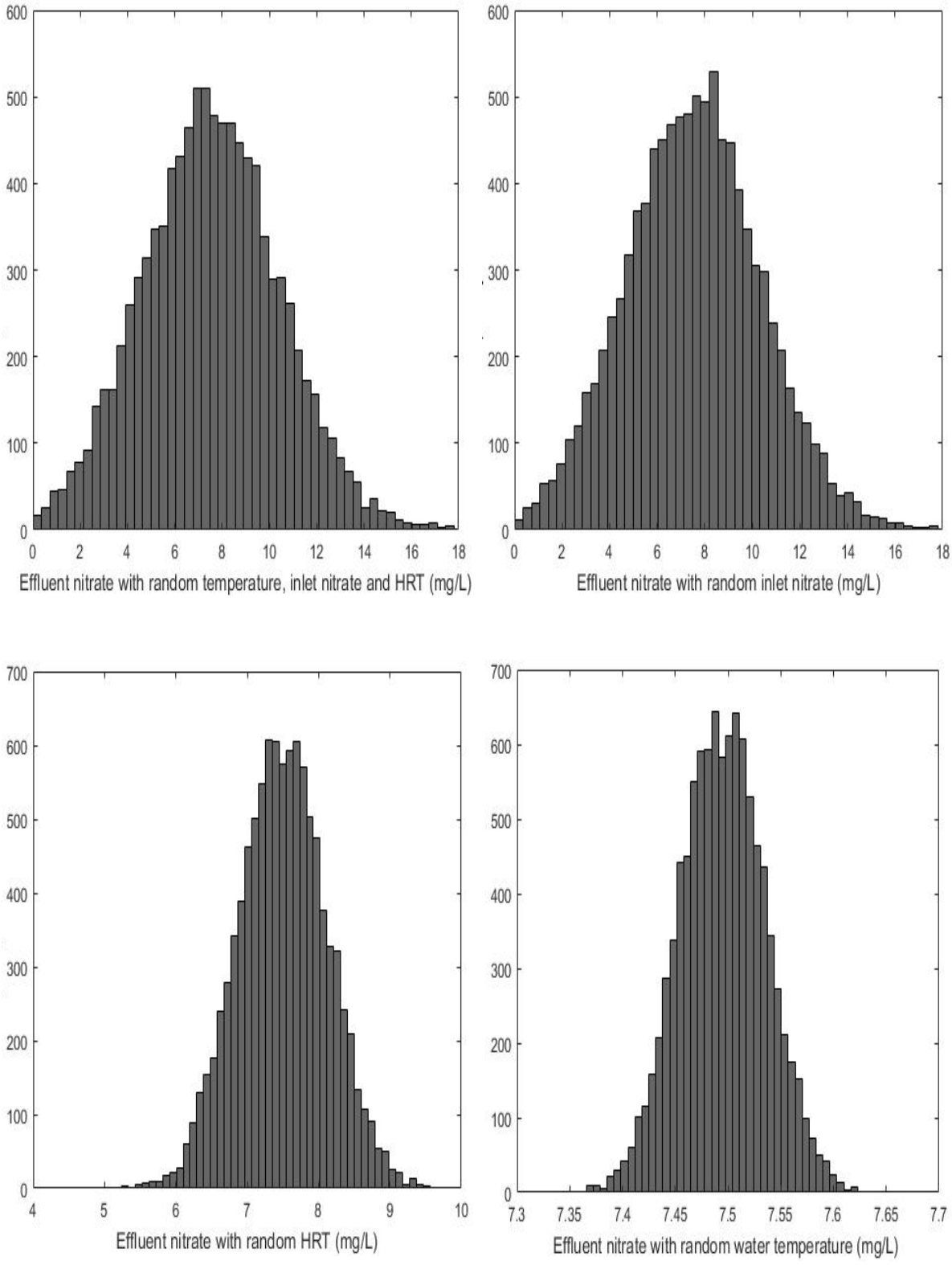

Figure 4.8: Frequency distributions of randomly generated effluent NO_3^- concentrations

variable stated above, effluent NO_3^- concentrations were simulated based on a multivariate probability distribution for parameters of interest as well. (Figure 4.8). STD values estimated for the univariate sensitivity analysis (varying influent NO_3^-, water temperature and HRT) are 2.85, 0.04 and 0.62 respectively, and for the multivariate distribution is 2.92. The multivariate distribution can be assumed to represent the overall prediction error, thus combined effects of all uncertainties in characterizing the evaluated model. The STDs and frequency distributions of randomly created outputs presented in Figure 4.7 may suggest that the denitrification process in the bioreactor is primarily subject to the changes in influent NO_3^- concentration, then HRT while the effect of temperature did not seem to statistically significant with a comparatively lower STD of 0.04. This finding could be resulted from the fact that monitored water temperature elevated in a narrow range of approximately from 8 to 11°C through observation period, thus it led to a limited distribution for parent domain of temperature.

The sensitivity of the first model against model input parameters was, furthermore, investigated through increasing the values of observed (influent NO_3^-, temperature) and predicted (drainage effluent) parameters individually by +10%. The most influential variables were then determined in line with the alteration in the root mean square error (RMSE) (Eq. 4.3) between the observed and predicted effluent NO_3^- concentrations (Table 4.1).

$$RMSE = \sqrt{\frac{\sum(C_{obs} - C_{sim})^2}{N}} \tag{4.3}$$

Table 4.1: The sensitivity of the denitrification process to model input parameters

Parameter	Unit	Average value	+10% change	RMSE with original input	RMSE with +10% change	Change in RMSE %
Influent nitrate	mg/L	7.94	8.73	2.10	2.61	24.37
HRT	hours	5.02	5.52	2.10	2.49	18.64
Temperature	°C	9.67	10.64	2.10	2.48	18.33

RMSE-based sensitivity analysis are in agreement with Monte Carlo model outputs in terms of the estimated influences of each model input parameters on the nitrate removal process. In most of the simulation models, only a limited number of input parameters exhibit major impact on the output. According to such employed procedure for parameter-specific sensitivity analysis, the most influential parameter is influent NO_3-N followed by HRT and water temperature, respectively, as could be concluded in accordance with statistical distributions of randomly generated outputs.

CHAPTER 5. CONCLUSIONS AND FUTURE DIRECTIONS

At conclusion of this field-scale study, the monitored denitrifying bioreactor was effective in nitrate reduction from tile drainage water at various hydraulic retention times during winter months. As expected, the mean NO_3^- percent removal (26 %) was lower than reported values for the bioreactors receiving relatively warmer drainage water. However, no significant correlation was found between increasing tile water temperature and increased NO_3^- percent removals achieved through study period as a consequence of the narrow temperature range (8-11°C). Hence, there was an insufficient monitoring data to evaluate the temperature effect on denitrification kinetics in the bioreactor. Long-term data are needed to determine the temperature dependency of NO_3^- removal process in different NO_3^- loading rates and climatic settings.

This study served as one of the few that simulated both bioreactor performance and NO_3^- concentration profile along the length of the denitrification bed. A new model for NO_3^- removal process in the bioreactor was developed using predicted drainage discharge by Drainmod. Furthermore, MIN3P code was executed to simulate NO_3^- concentrations in the effluent and monitoring wells. The model results was benchmarked against the observed NO_3^- in the outlet control structure, and resulted in a Nash-Sutcliffe efficiency coefficient (NSE) value of 0.506 that meets one of the pre-specified model evaluation metrics (NSE>0.5, R^2 >0.6). Further field-scale studies are still needed in order to examine the applicability of the model under various environmental settings. The sensitivity analysis was performed to examine the influences of the key input parameters on the NO_3^- removal

model. The model output is substantially sensitive to influent NO_3^-, followed by hydraulic retention time, while alterations in water temperature have a relatively low effect considering frequency distributions of randomly generated outcomes based on Monte Carlo simulation. On the other hand, the NSE value computed in validation of MIN3P code was slightly below the coefficient of determination criteria (NSE = 0.043, R^2 = 0.416). These comparatively low (still useful in developing reliable predictions) MIN3P simulation performance metrics could be attributed to some of the model input parameters, especially those that are currently unavailable for the study area and assumed to be equal to the values reported in the similar studies (rate expressions, horizontal hydraulic conductivity, effective porosity). Thus, the predictive power of the model is likely to be higher with more field-specific parameters. The MIN3P code executed to simulate NO_3^- concentration profile along the length of the bioreactor suggest that denitrification occurs efficiently within first 2.6 m of the system. This model result would be associated with increased reaction rates over time near the upstream of the bioreactor because of the biomass growth and accumulation. Spatial analysis for NO_3^- and biomass concentrations through the length of the bioreactor could be performed following long-term sampling from monitoring wells as well as control structures in order to test hypotheses mentioned above.

Bibliography

Addy, K., Gold, A. J., Christianson, L. E., David, M. B., Schipper, L. A., & Ratigan, N. A. (2016). Denitrifying Bioreactors for Nitrate Removal: A Meta-Analysis. *Journal of Environment Quality*, *45*(3), 873. https://doi.org/10.2134/jeq2015.07.0399

Bakhsh, A., Kanwar, R. S., Pederson, C., & Bailey, T. B. (2007). N-source effects on temporal distribution of NO3-N leaching losses to subsurface drainage water. *Water, Air, and Soil Pollution*, *181*(1–4), 35–50. https://doi.org/10.1007/s11270-006-9274-z

Bell, N., Cooke, R. A. C., Olsen, T., David, M. B., & Hudson, R. (2015). Characterizing the Performance of Denitrifying Bioreactors during Simulated Subsurface Drainage Events. *Journal of Environment Quality*, *44*(5), 1647. https://doi.org/10.2134/jeq2014.04.0162

Blowes, D. W., Robertson, W. D., Ptacek, C. J., & Merkley, C. (1994). Removal of agricultural nitrate from tile-drainage effluent water using in-line bioreactors. *Journal of Contaminant Hydrology*, *15*(3), 207–221. https://doi.org/10.1016/0169-7722(94)90025-6

Burt, T. P., Heathwaite, A. L. (A. L., & Trudgill, S. T. (Stephen T. (1993). *Nitrate : processes, patterns, and management*. J. Wiley. Retrieved from https://catalogue.nla.gov.au/Record/2691446

Cambardella, C. A., Moorman, T. B., Jaynes, D. B., Hatfield, J. L., Parkin, T. B., Simpkins, W. W., & Karlen, D. L. (1999). Water Quality in Walnut Creek Watershed: Nitrate-Nitrogen in Soils, Subsurface Drainage Water, and Shallow Groundwater. *Journal of Environment Quality*, *28*(1), 25. https://doi.org/10.2134/jeq1999.00472425002800010003x

Cameron, S. G., & Schipper, L. A. (2010). Nitrate removal and hydraulic performance of organic carbon for use in denitrification beds. *Ecological Engineering*, *36*(11), 1588–1595. https://doi.org/10.1016/j.ecoleng.2010.03.010

Christianson, L. (2011). Design and performance of denitrification bioreactors for agricultural drainage. *Graduate Theses and Dissertations*. https://doi.org/https://doi.org/10.31274/etd-180810-1436

Christianson, L., Bhandari, A., & Helmers, M. J. (2011). Pilot-Scale evaluation of denitrification drainage bioreactors: Reactor geometry and performance. *Journal of Environmental Engineering*, *137*(4), 213–220. https://doi.org/10.1061/(ASCE)EE.1943-7870.0000316

Christianson, L., Christianson, R., Helmers, M., & Bhandari, A. (2010). Technical Note: Hydraulic Property Determination of Denitrifying Bioreactor Fill Media. *Soil & Water Division of ASABE*, *26*(5), 849–854. Retrieved from http://lib.dr.iastate.edu/abe_eng_pubs

Christianson, L. E., Bhandari, A., & Helmers, M. J. (2012). A practice-oriented review of woodchip bioreactors for subsurface agricultural drainage. *Applied Engineering in Agriculture*. https://doi.org/10.13031/2013.42479

Christianson, L., & Helmers, M. (2011). Woodchip bioreactors for nitrate in agricultural drainage. *Iowa State University Extension Publication PMR 1008.*, (October), 1–4. Retrieved from https://lib.dr.iastate.edu/extension_ag_pubs/85

Chun, J. A., Cooke, R. A., Eheart, J. W., & Cho, J. (2010). Estimation of flow and transport parameters for woodchip-based bioreactors: II. field-scale bioreactor. *Biosystems Engineering*, *105*(1), 95–102. https://doi.org/10.1016/j.biosystemseng.2009.09.018

Cooke, Doheny, & Hirschi. (2001). Bio-reactors for edge-of-field treatment of tile outflow. *ASAE International Meeting*, *0300*(xx), 1–17. https://doi.org/10.13031/2013.7373

David, M. B., Gentry, L. E., Cooke, R. A., & Herbstritt, S. M. (2016). Temperature and Substrate Control Woodchip Bioreactor Performance in Reducing Tile Nitrate Loads in East-Central Illinois. *Journal of Environment Quality*, *45*(3), 822. https://doi.org/10.2134/jeq2015.06.0296

Della Rocca, C., Belgiorno, V., & Meriç, S. (2005). Cotton-supported heterotrophic denitrification of nitrate-rich drinking water with a sand filtration post-treatment. *Water SA*, *31*(2), 229–236. https://doi.org/10.4314/wsa.v31i2.5177

Devito, K. J., Fitzgerald, D., Hill, A. R., & Aravena, R. (2000). Nitrate Dynamics in Relation to Lithology and Hydrologic Flow Path in a River Riparian Zone. *Journal of Environment Quality*, *29*(4), 1075. https://doi.org/10.2134/jeq2000.00472425002900040007x

Dörsch, P., Braker, G., & Bakken, L. R. (2012). Community-specific pH response of denitrification: Experiments with cells extracted from organic soils. *FEMS Microbiology Ecology*, *79*(2), 530–541. https://doi.org/10.1111/j.1574-6941.2011.01233.x

Downie, A., Crosky, A., & Munroe, P. (2009). Physical Properties of Biochar. Introduction. *Biochar for Environmental Management: Science and Technology*, 13–32. https://doi.org/10.4324/9781849770552-9

Drablos, C.J.W., and R. M. (1984). Illinois Drainage Guide, Circular 122b, 46. Retrieved from http://www.wq.illinois.edu/dg/subsurface.htm

Drtil, M., Németh, P., Buday, J., Bodík, I., & Hutňan, M. (1998). Regulation of Denitrification Using Continually Measured ORP and pH Signal. *Chem. Papers*, *53*(1), 75–81. Retrieved from https://www.chempap.org/file_access.php?file=531a75.pdf

Elgood, Z., Robertson, W. D., Schiff, S. L., & Elgood, R. (2010). Nitrate removal and greenhouse gas production in a stream-bed denitrifying bioreactor. *Ecological Engineering*, *36*(11), 1575–1580. https://doi.org/10.1016/j.ecoleng.2010.03.011

Follett, J. R., Follett, R. F., & Herz, W. C. (2010). Environmental and human impacts of reactive nitrogen. In *Advances in Nitrogen Management for Water Quality* (p. 1–37; 1). Retrieved from https://www.swcs.org/media/cms/ANM1_3B940A0B78CF7.pdf

Ghane, E., Fausey, N. R., & Brown, L. C. (2015). Modeling nitrate removal in a denitrification bed. *Water Research*, *71*, 294–305. https://doi.org/10.1016/j.watres.2014.10.039

Gibert, O., Pomierny, S., Rowe, I., & Kalin, R. M. (2008). Selection of organic substrates as potential reactive materials for use in a denitrification permeable reactive barrier (PRB). *Bioresource Technology*, *99*(16), 7587–7596. https://doi.org/10.1016/J.BIORTECH.2008.02.012

Greenan, C. M., Moorman, T. B., Kaspar, T. C., Parkin, T. B., & Jaynes, D. B. (2006). Comparing Carbon Substrates for Denitrification of Subsurface Drainage Water. *Journal of Environment Quality*, *35*(3), 824. https://doi.org/10.2134/jeq2005.0247

Grohman, T. A. (2017). Proposal of an Automated Workflow for Appropriate Tile Drainage Simulation in Denitrifying Bioreactor Planning and Design. Master's thesis, Department of Biological and Ecological Engineering at Oregon State University

Hageman, R. H., & Hucklesby, D. P. (1971). Nitrate Reductase from Higher Plants. *Methods in Enzymology*, *23*(C), 491–503. https://doi.org/10.1016/S0076-6879(71)23121-9

Hassanpour, B., Giri, S., Pluer, W. T., Steenhuis, T. S., & Geohring, L. D. (2017). Seasonal performance of denitrifying bioreactors in the Northeastern United States: Field trials. *Journal of Environmental Management*, *202*, 242–253. https://doi.org/10.1016/j.jenvman.2017.06.054

Havill, N. P., Elkinton, J., Andersen, J. C., Hagen, S. B., Broadley, H. J., Boettner, G. J., &

Caccone, A. (2017). Asymmetric hybridization between non-native winter moth, Operophtera brumata (Lepidoptera: Geometridae), and native Bruce spanworm, Operophtera bruceata, in the Northeastern United States, assessed with novel microsatellites and SNPs. *Bulletin of Entomological Research*, *107*(2), 241–250. https://doi.org/10.1017/S0007485316000857

Healy, M. G., Ibrahim, T. G., Lanigan, G. J., Serrenho, A. J., & Fenton, O. (2012). Nitrate removal rate, efficiency and pollution swapping potential of different organic carbon media in laboratory denitrification bioreactors. *Ecological Engineering*, *40*, 198–209. https://doi.org/10.1016/j.ecoleng.2011.12.010

Hobbs, J. K., Jiao, W., Easter, A. D., Parker, E. J., Schipper, L. A., & Arcus, V. L. (2013). Change in Heat Capacity for Enzyme Catalysis Determines Temperature Dependence of Enzyme Catalyzed Rates. *ACS Chemical Biology*, *8*(11), 2388–2393. https://doi.org/10.1021/cb4005029

Hoover, N. L., Bhandari, A., Soupir, M. L., & Moorman, T. B. (2016). Woodchip Denitrification Bioreactors: Impact of Temperature and Hydraulic Retention Time on Nitrate Removal. *Journal of Environment Quality*, *45*(3), 803. https://doi.org/10.2134/jeq2015.03.0161

Hoover, N. L., Soupir, M. L., VanDePol, R. D., Goode, T. R., & Law, J. Y. (2017). Pilot-scale denitrification bioreactors for replicated field research. *Applied Engineering in Agriculture*, *33*(1), 83–90. https://doi.org/10.13031/aea.11736

Ikenberry, C. D., Soupir, M. L., Schilling, K. E., Jones, C. S., & Seeman, A. (2014). Nitrate-Nitrogen Export: Magnitude and Patterns from Drainage Districts to Downstream River Basins. *Journal of Environment Quality*, *43*(6), 2024. https://doi.org/10.2134/jeq2014.05.0242

Ima, C. S., & Mann, D. D. (2007). Physical Properties of Woodchip : Compost Mixtures used as Biofilter Media. *Agricultural Engineering International*, *IX*, 1–7. Retrieved from https://ecommons.cornell.edu/bitstream/handle/1813/10618/BC 07 005 Mann final 7Sept2007.pdf?sequence=1

Jacinthe, P.-A., Groffman, P. M., Gold, A. J., & Mosier, A. (1998). Patchiness in Microbial Nitrogen Transformations in Groundwater in a Riparian Forest. *Journal of Environment Quality*, *27*(1), 156. https://doi.org/10.2134/jeq1998.00472425002700010022x

Jaynes, D. B., Kaspar, T. C., Moorman, T. B., & Parkin, T. B. (2008). In Situ Bioreactors and Deep Drain-Pipe Installation to Reduce Nitrate Losses in Artificially Drained Fields. *Journal of Environment Quality*, *37*(2), 429. https://doi.org/10.2134/jeq2007.0279

Kellman, L. M. (2005). A study of tile drain nitrate - ?15N values as a tool for assessing nitrate sources in an agricultural region. *Nutrient Cycling in Agroecosystems*, *71*(2), 131–137. https://doi.org/10.1007/s10705-004-1925-0

Knowles, R. (1982). Denitrification. *Microbiological Reviews*, *46*(1), 43–70. Retrieved from http://www.ncbi.nlm.nih.gov/pubmed/7045624

Korom, S. F. (1992). Natural denitrification in the saturated zone: A review. *Water Resources Research*, *28*(6), 1657–1668. https://doi.org/10.1029/92WR00252

Korom, S. F., Schlag, A. J., Schuh, W. M., & Schlag, A. K. (2005). In situ mesocosms: Denitrification in the Elk Valley aquifer. *Ground Water Monitoring and Remediation*, *25*(1), 79–89. https://doi.org/10.1111/j.1745-6592.2005.0003.x

L. Christianson, A. Bhandari, M. Helmers, K. Kult, T. Sutphin, & R. Wolf. (2012). Performance Evaluation of Four Field-Scale Agricultural Drainage Denitrification Bioreactors in Iowa. *Transactions of the ASABE*, *55*(6), 2163–2174. https://doi.org/10.13031/2013.42508

Laudone, G. M., Matthews, G. P., Bird, N. R. A., Whalley, W. R., Cardenas, L. M., & Gregory, A. S. (2011). A model to predict the effects of soil structure on denitrification and N2O emission. *Journal of Hydrology*, *409*(1–2), 283–290. https://doi.org/10.1016/j.jhydrol.2011.08.026

Lee, M. S., Lee, K. K., Hyun, Y., Clement, T. P., & Hamilton, D. (2006). Nitrogen transformation and transport modeling in groundwater aquifers. *Ecological Modelling*, *192*(1–2), 143–159. https://doi.org/10.1016/j.ecolmodel.2005.07.013

Likens, G. E., Driscoll, C. T., & Buso, D. C. (1996). Long-Term Effects of Acid Rain: Response and Recovery of a Forest Ecosystem. *Science*, *272*(5259), 244–246. https://doi.org/10.1126/science.272.5259.244

Logan, T. J. (1993). Agricultural best management practices for water pollution control: current issues. *Agriculture, Ecosystems & Environment*, *46*(1–4), 223–231. https://doi.org/10.1016/0167-8809(93)90026-L

Malia Appleford, J., Rodriguez, L. F., Cooke, R. A. C., Zhang, Y., Kent, A. D., & Zilles, J. (2008). Characterization of microorganisms contributing to denitrification in tile drain biofilters in illinois. In *American Society of Agricultural and Biological Engineers Annual International Meeting 2008, ASABE 2008* (Vol. 9, pp. 5605–5614). American Society of Agricultural and Biological Engineers. https://doi.org/10.13031/2013.24655

Mayer, K. U., Frind, E. O., & Blowes, D. W. (2002). Multicomponent reactive transport modeling in variably saturated porous media using a generalized formulation for kinetically controlled reactions. *Water Resources Research*, *38*(9), 13-1-13–21.

https://doi.org/10.1029/2001WR000862

Melching, C., & Flores, H. (1999). Reaeration Equations Derived from U.S. Geological Survey Database. *Journal of Environmental Engineering*, *125*(5), 407–414. https://doi.org/10.1061/(ASCE)0733-9372(1999)125:5(407)

Mineral commodity summaries 2015. (2015). *Mineral Commodity Summaries*. Reston, VA. https://doi.org/10.3133/70140094

Miranda, K. M., Espey, M. G., & Wink, D. A. (2001). A rapid, simple spectrophotometric method for simultaneous detection of nitrate and nitrite. *Nitric Oxide - Biology and Chemistry*, *5*(1), 62–71. https://doi.org/10.1006/niox.2000.0319

Mo, H., Oleszkiewicz, J. A., Cicek, N., & Rezania, B. (2005). Incorporating membrane gas diffusion into a membrane bioreactor for hydrogenotrophic denitrification of groundwater. *Water Science and Technology*, *51*(6–7), 357–364. Retrieved from http://www.ncbi.nlm.nih.gov/pubmed/16003997

Molins, S., Greskowiak, J., Wanner, C., & Mayer, K. U. (2015). A benchmark for microbially mediated chromium reduction under denitrifying conditions in a biostimulation column experiment. *Computational Geosciences*, *19*(3), 479–496. https://doi.org/10.1007/s10596-014-9432-0

Moorman, T. B., Parkin, T. B., Kaspar, T. C., & Jaynes, D. B. (2010). Denitrification activity, wood loss, and N2O emissions over 9 years from a wood chip bioreactor. *Ecological Engineering*, *36*(11), 1567–1574. https://doi.org/10.1016/j.ecoleng.2010.03.012

Mualem, Y. (1976). A new model for predicting the hydraulic conductivity of unsaturated porous media. *Water Resources Research*, *12*(3), 513–522. https://doi.org/10.1029/WR012i003p00513

Mueller, D. K., & Spahr, N. E. (2006). Nutrients in Streams and Rivers Across the Nation — 1992–2001 Scientific Investigations Report 2006–5107. *Nutrients in Streams and Rivers Across the Nation*. Retrieved from http://water.usgs.gov/nawqa/studyu.html

N. Brady, R. W. (2002). The Nature and Properties of Soils, 13th Edition.By N. C. Brady and R. R. Weil. *Agroforestry Systems*, *54*(3), 249. https://doi.org/10.1023/A:1016012810895

Nash, J. E., & Sutcliffe, J. V. (1970). River flow forecasting through conceptual models part I - A discussion of principles. *Journal of Hydrology*, *10*(3), 282–290. https://doi.org/10.1016/0022-1694(70)90255-6

NRCS-USDA. (2015). Conservation practice standard denitrifying bioreactor. Code 605.

Retrieved December 3, 2018, from www.nrcs.usda.gov

P. W. van Driel, W. D. Robertson, & L. C. Merkley. (2006). DENITRIFICATION OF AGRICULTURAL DRAINAGE USING WOOD-BASED REACTORS. *Transactions of the ASABE*, *49*(2), 565–573. https://doi.org/10.13031/2013.20391

Pabich, W. J., Valiela, I., & Hemond, H. F. (2001). Relationship between DOC concentration and vadose zone thickness and depth below water table in groundwater of Cape Cod, U.S.A. *Biogeochemistry*, *55*(3), 247–268. https://doi.org/10.1023/A:1011842918260

Paré, D., Boutin, R., Larocque, G. R., & Raulier, F. (2006). Effect of temperature on soil organic matter decomposition in three forest biomes of eastern Canada. *Canadian Journal of Soil Science*, *86*(Special Issue), 247–256. https://doi.org/10.4141/S05-084

Porter, M. D., Andrus, J. M., Bartolerio, N. A., Rodriguez, L. F., Zhang, Y., Zilles, J. L., & Kent, A. D. (2015). Seasonal Patterns in Microbial Community Composition in Denitrifying Bioreactors Treating Subsurface Agricultural Drainage. *Microbial Ecology*, *70*(3), 710–723. https://doi.org/10.1007/s00248-015-0605-8

Qiu, X. C., Liu, G. P., & Zhu, Y. Q. (1987). Determination of water-soluble ammonium ion in soil by spectrophotometry. *The Analyst*, *112*(6), 909–911. https://doi.org/10.1039/an9871200909

R. W. Skaggs, M. A. Youssef, & G. M. Chescheir. (2012). DRAINMOD: Model Use, Calibration, and Validation. *Transactions of the ASABE*, *55*(4), 1509–1522. https://doi.org/10.13031/2013.42259

Rabalais, N. N., Turner, R. E., Diaz, R. J., & Justic, D. (2009). Global change and eutrophication of coastal waters. *ICES Journal of Marine Science*, *66*(7), 1528–1537. https://doi.org/10.1093/icesjms/fsp047

Rivett, M. O., Buss, S. R., Morgan, P., Smith, J. W. N., & Bemment, C. D. (2008). Nitrate attenuation in groundwater: A review of biogeochemical controlling processes. *Water Research*, *42*(16), 4215–4232. https://doi.org/10.1016/j.watres.2008.07.020

Robertson, G. P., & Groffman, P. M. (2015). Nitrogen Transformations. In *Soil Microbiology, Ecology and Biochemistry* (pp. 421–446). https://doi.org/10.1016/B978-0-12-415955-6.00014-1

Robertson, L. A., Cornelisse, R., De Vos, P., Hadioetomo, R., & Kuenen, J. G. (1989). Aerobic denitrification in various heterotrophic nitrifiers. *Antonie van Leeuwenhoek*, *56*(4), 289–299. https://doi.org/10.1007/BF00443743

Robertson, W. D. (2010). Nitrate removal rates in woodchip media of varying age.

Ecological Engineering, *36*(11), 1581–1587. https://doi.org/10.1016/j.ecoleng.2010.01.008

Robertson, W. D., Blowes, D. W., Ptacek, C. J., & Cherry, J. A. (2000). Long-term performance of in situ reactive barriers for nitrate remediation. *Ground Water*, *38*(5), 689–695. https://doi.org/10.1111/j.1745-6584.2000.tb02704.x

Robertson, W. D., Ford, G. I., & Lombardo, P. S. (2005). WOOD−BASED FILTER FOR NITRATE REMOVAL IN SEPTIC SYSTEMS. *Transactions of the ASABE*, *48*(1), 121–128. https://doi.org/10.13031/2013.17954

Robertson, W. D., & Merkley, L. C. (2009). In-Stream Bioreactor for Agricultural Nitrate Treatment. *Journal of Environment Quality*, *38*(1), 230. https://doi.org/10.2134/jeq2008.0100

Royer, T. V, David, M. B., & Gentry, L. E. (2006). Timing of riverine export of nitrate and phosphorus from agricultural watersheds in Illinois: implications for reducing nutrient loading to the Mississippi River. *Environmental Science & Technology*, *40*(13), 4126–4131. Retrieved from http://www.ncbi.nlm.nih.gov/pubmed/16856726

Rust, C. M., Aelion, C. M., & Flora, J. R. V. (2000). Control of pH during denitrification in subsurface sediment microcosms using encapsulated phosphate buffer. *Water Research*, *34*(5), 1447–1454. https://doi.org/10.1016/S0043-1354(99)00287-0

Saliling, W. J. B., Westerman, P. W., & Losordo, T. M. (2007). Wood chips and wheat straw as alternative biofilter media for denitrification reactors treating aquaculture and other wastewaters with high nitrate concentrations. *Aquacultural Engineering*, *37*(3), 222–233. https://doi.org/10.1016/j.aquaeng.2007.06.003

Santhi, C., Hauck, L. M., Arnold, J. G., Williams, J. R., Dugas, W. A., & Srinivasan, R. (2007). VALIDATION OF THE SWAT MODEL ON A LARGE RWER BASIN WITH POINT AND NONPOINT SOURCES. *Journal of the American Water Resources Association*, *37*(5), 1169–1188. https://doi.org/10.1111/j.1752-1688.2001.tb03630.x

Scavia, D., & Bricker, S. B. (2006). Coastal eutrophication assessment in the United States. In *Biogeochemistry* (Vol. 79, pp. 187–208). Springer. https://doi.org/10.1007/s10533-006-9011-0

Schaap, M. G., Leij, F. J., & Van Genuchten, M. T. (2001). Rosetta: A computer program for estimating soil hydraulic parameters with hierarchical pedotransfer functions. *Journal of Hydrology*, *251*(3–4), 163–176. https://doi.org/10.1016/S0022-1694(01)00466-8

Schimel, J. P., & Gulledge, J. (1998). Microbial community structure and global trace gases. *Global Change Biology*, *4*(7), 745–758. https://doi.org/10.1046/j.1365-

2486.1998.00195.x

Schindler, D. W. (1990). Experimental Perturbations of Whole Lakes as Tests of Hypotheses concerning Ecosystem Structure and Function. *Oikos*, *57*(1), 25. https://doi.org/10.2307/3565733

Schindler, D. W., Turner, M. A., & Hesslein, R. H. (1985). Acidification and alkalinization of lakes by experimental addition of nitrogen compounds. *Biogeochemistry*, *1*(2), 117–133. https://doi.org/10.1007/BF02185037

Schipper, L. A., Hobbs, J. K., Rutledge, S., & Arcus, V. L. (2014). Thermodynamic theory explains the temperature optima of soil microbial processes and high Q10 values at low temperatures. *Global Change Biology*, *20*(11), 3578–3586. https://doi.org/10.1111/gcb.12596

Schipper, L. A., Robertson, W. D., Gold, A. J., Jaynes, D. B., & Cameron, S. C. (2010, November 1). Denitrifying bioreactors-An approach for reducing nitrate loads to receiving waters. *Ecological Engineering*. Elsevier. https://doi.org/10.1016/j.ecoleng.2010.04.008

Schipper, L., & Vojvodić-Vuković, M. (1998). Nitrate removal from groundwater using a denitrification wall amended with sawdust: Field trial. *Journal of Environment Quality*. https://doi.org/10.2134/jeq1998.00472425002700030025x

Schmidt, C. A., & Clark, M. W. (2013). Deciphering and modeling the physicochemical drivers of denitrification rates in bioreactors. *Ecological Engineering*, *60*, 276–288. https://doi.org/10.1016/j.ecoleng.2013.07.041

Seitzinger, S., Harrison, J. A., Böhlke, J. K., Bouwman, A. F., Lowrance, R., Peterson, B., … Van Drecht, G. (2006). Denitrification across landscapes and waterscapes: a synthesis. *Ecological Applications : A Publication of the Ecological Society of America*, *16*(6), 2064–2090. Retrieved from http://www.ncbi.nlm.nih.gov/pubmed/17205890

Shih, R., Robertson, W. D., Schiff, S. L., & Rudolph, D. L. (2011). Nitrate Controls Methyl Mercury Production in a Streambed Bioreactor. *Journal of Environment Quality*, *40*(5), 1586. https://doi.org/10.2134/jeq2011.0072

Skaggs, R. (1978). A water management model for shallow water table soils. *North Carolina. University. Water Resources Research*

Soares, M. I. M., & Abeliovich, A. (1998). Wheat straw as substrate for water denitrification. *Water Research*, *32*(12), 3790–3794. https://doi.org/10.1016/S0043-1354(98)00136-5

Song, S. H., Yeom, S., Choi, S., & Yoo, Y. J. (2003). *Effect of oxidation-reduction potential on denitrification by Ochrobactrum anthropi SY509*. *Journal of Microbiology and Biotechnology* (Vol. 13).

Stenger, R., Clague, J., Woodward, S., Moorhead, B., Wilson, S., Shokri, A., … Canard, H. (2013). Denitrification - the key component of a groundwater system's assimilative capacity for nitrate. In *Fertiliser & Lime Research Centre Workshop Proceedings* (pp. 1–11). Retrieved from https://www.massey.ac.nz/~flrc/workshops/13/Manuscripts/Paper_Stenger_2013.pdf

van Verseveld, W. J., McDonnell, J. J., & Lajtha, K. (2009). The role of hillslope hydrology in controlling nutrient loss. *Journal of Hydrology*, *367*(3–4), 177–187. https://doi.org/10.1016/J.JHYDROL.2008.11.002

Verma, S., Bhattarai, R., Goodwin, G., Cooke, R., & Chun, J. A. (2010). Evaluation of Conservation Drainage Systems in Illinois – Bioreactors. In *2010 ASABE Annual International Meeting* (p. Paper Number: 1009894). American Society of Agricultural and Biological Engineers. https://doi.org/10.13031/2013.30015

Warneke, S., Schipper, L. A., Bruesewitz, D. A., McDonald, I., & Cameron, S. (2011). Rates, controls and potential adverse effects of nitrate removal in a denitrification bed. *Ecological Engineering*, *37*(3), 511–522. https://doi.org/10.1016/j.ecoleng.2010.12.006

Warneke, S., Schipper, L. A., Matiasek, M. G., Scow, K. M., Cameron, S., Bruesewitz, D. A., & McDonald, I. R. (2011). Nitrate removal, communities of denitrifiers and adverse effects in different carbon substrates for use in denitrification beds. *Water Research*, *45*(17), 5463–5475. https://doi.org/10.1016/j.watres.2011.08.007

Wieben, C. M., Baker, R. J., & Nicholson, R. S. (2013). *Nutrient concentrations in surface water and groundwater, and nitrate source identification using stable isotope analysis, in the Barnegat Bay-Little Egg Harbor watershed, New Jersey, 2010–11: U.S. Geological Survey Scientific Investigations Report 2012–5*. Retrieved from https://pubs.usgs.gov/sir/2012/5287/support/sir2012-5287.pdf

Woli, K. P., David, M. B., Cooke, R. A., McIsaac, G. F., & Mitchell, C. A. (2010). Nitrogen balance in and export from agricultural fields associated with controlled drainage systems and denitrifying bioreactors. *Ecological Engineering*, *36*(11), 1558–1566. https://doi.org/10.1016/j.ecoleng.2010.04.024

Zou, X. M., Ruan, H. H., Fu, Y., Yang, X. D., & Sha, L. Q. (2005). Estimating soil labile organic carbon and potential turnover rates using a sequential fumigation-incubation procedure. *Soil Biology and Biochemistry*, *37*(10), 1923–1928. https://doi.org/10.1016/j.soilbio.2005.02.028

APPENDIX

Table A.1: Nitrate-N concentrations used to estimate percent removal and volumetric load reduction rates

Date	Influent Nitrate(mg/l)	Effluent Nitrate(mg/l)	Load Reduction Rate (g N/ m^3/d)	Percent Removal (%)
12/7/2017	12.53	12.07	7.60	3.64
12/9/2017	12.41	12.28	1.24	1.00
12/10/2017	12.03	11.70	2.63	2.76
12/11/2017	12.53	11.87	4.30	5.30
12/13/2017	11.04	10.83	0.98	1.88
12/14/2017	10.87	9.00	7.63	17.18
12/15/2017	11.70	11.16	1.93	4.61
12/16/2017	11.66	10.46	3.80	10.32
12/17/2017	11.12	5.93	14.40	46.64
12/19/2017	9.67	6.18	7.57	36.05
12/20/2017	6.14	5.15	2.03	16.22
12/21/2017	11.95	3.44	15.09	71.18
12/22/2017	5.93	4.61	1.86	22.38
12/23/2017	5.27	4.40	3.11	16.54
12/24/2017	9.50	5.85	50.95	38.43
12/30/2017	6.89	4.52	29.56	34.34
12/31/2017	8.88	6.27	27.10	29.44
1/5/2018	4.85	2.28	22.15	52.99
1/6/2018	9.05	6.02	21.55	33.49
1/7/2018	9.21	6.85	13.86	25.68
1/8/2018	8.51	8.38	0.81	1.46
1/9/2018	10.75	6.93	41.91	35.52
1/10/2018	7.47	5.15	24.05	31.11
1/11/2018	2.32	1.62	5.70	30.36
1/12/2018	7.97	7.39	5.15	7.29
1/14/2018	6.35	3.53	40.04	44.44
1/15/2018	5.77	5.15	12.99	10.79
1/16/2018	6.43	5.89	13.86	8.39
1/17/2018	4.81	1.33	57.05	72.41
1/19/2018	6.97	4.32	24.12	38.10
1/27/2018	10.46	4.40	107.16	57.94
1/28/2018	10.66	6.14	168.96	42.41
1/29/2018	7.97	6.43	60.45	19.27
1/30/2018	8.92	7.93	37.84	11.16
1/31/2018	8.76	6.64	60.11	24.17
2/1/2018	6.97	6.47	9.98	7.14

2/3/2018	10.12	4.61	88.11	54.51
2/4/2018	4.07	3.65	5.27	10.20
2/5/2018	6.93	5.19	16.85	25.15
2/6/2018	4.69	2.86	12.87	38.94
2/9/2018	6.97	4.32	5.37	38.10
2/12/2018	3.86	3.44	-	10.75
2/13/2018	10.29	6.31	-	38.71
2/14/2018	7.59	4.77	-	37.16

Table A.2: Simulated effluent Nitrate-N concentrations, monitored water temperature, and predicted drainage discharge

Date	Water Temperature (°C)	Drainage Discharge (cm/d)	Effluent Nitrate by the Model (mg/L)	Effluent Nitrate by MIN3P (mg/L)
12/7/2017	11.23	0.46	12.25	9.55
12/9/2017	11.04	0.27	11.95	9.42
12/10/2017	10.94	0.22	11.84	8.98
12/11/2017	10.74	0.18	11.36	9.47
12/13/2017	10.35	0.13	10.91	8.01
12/14/2017	10.25	0.11	10.04	7.83
12/15/2017	9.96	0.10	9.78	8.68
12/16/2017	9.86	0.09	10.48	8.67
12/17/2017	9.96	0.08	10.25	8.10
12/19/2017	8.18	0.06	9.72	6.69
12/20/2017	9.17	0.06	7.95	3.31
12/21/2017	9.57	0.05	4.05	8.92
12/22/2017	9.57	0.04	9.30	3.12
12/23/2017	8.87	0.10	4.99	2.52
12/24/2017	9.07	0.38	5.02	6.50
12/30/2017	9.57	0.34	4.52	4.00
12/31/2017	9.27	0.28	6.54	5.90
1/5/2018	8.58	0.24	4.48	0.92
1/6/2018	9.17	0.20	4.36	6.09
1/7/2018	9.17	0.16	8.45	6.27
1/8/2018	9.17	0.18	8.67	5.55
1/9/2018	9.27	0.30	8.18	7.72
1/10/2018	9.17	0.28	7.13	3.23
1/11/2018	10.06	0.22	6.98	0.37
1/12/2018	9.76	0.24	1.89	5.02
1/14/2018	9.57	0.39	5.55	3.49
1/15/2018	9.47	0.57	6.17	1.36
1/16/2018	9.47	0.70	5.63	3.61
1/17/2018	9.57	0.45	4.59	2.13
1/19/2018	9.37	0.25	1.64	4.07
1/27/2018	9.47	0.49	3.28	7.48
1/28/2018	9.96	1.02	10.56	7.66
1/29/2018	9.57	1.08	7.87	5.02
1/30/2018	9.57	1.04	7.87	5.97
1/31/2018	9.47	0.78	8.79	5.79

2/1/2018	9.47	0.55	8.57	4.07
2/3/2018	9.66	0.44	4.99	7.11
2/4/2018	9.76	0.35	3.77	0.60
2/5/2018	9.76	0.27	6.53	4.07
2/6/2018	9.76	0.19	4.15	0.98
2/9/2018	9.86	0.06	5.06	4.07
2/12/2018	9.86	0.00	-	-
2/13/2018	9.76	0.00	-	-
2/14/2018	9.27	0.00	-	-